Summer 8-2011

# Monte Carlo Simulation of Electron-Induced Air Fluorescence Utilizing Mobile Agents: A New Paradigm for Collaborative Scientific Simulation

Christopher Daniel Walker
*University of Southern Mississippi*

The University of Southern Mississippi

# MONTE CARLO SIMULATION OF ELECTRON-INDUCED AIR FLUORESCENCE UTILIZING MOBILE AGENTS: A NEW PARADIGM FOR COLLABORATIVE SCIENTIFIC SIMULATION

by

Christopher Daniel Walker

Abstract of a Dissertation
Submitted to the Graduate School
of The University of Southern Mississippi
in Partial Fulfillment of the Requirements
for the Degree of Doctor of Philosophy

August 2011

ABSTRACT

MONTE CARLO SIMULATION OF ELECTRON-INDUCED AIR FLUORESCENCE UTILIZING MOBILE AGENTS: A NEW PARADIGM FOR COLLABORATIVE SCIENTIFIC SIMULATION

by Christopher Daniel Walker

August 2011

A new paradigm for utilization of mobile agents in a modular architecture for scientific simulation is demonstrated through a case study involving Monte Carlo simulation of low energy electron interactions with molecular nitrogen gas. Design and development of Monte Carlo simulations for physical systems of moderate complexity can present a seemingly overwhelming endeavor. The researcher must possess or otherwise develop a thorough understanding the physical system, create mathematical and computational models of the physical system's components, and forge a simulation utilizing those models. While there is no single route between a collection of physical concepts and a Monte Carlo simulation based on those concepts, this work develops a new paradigm based on agent-oriented architecture and modular design principles through a case study in which interactions between electrons and molecules are simulated. A methodology that incorporates both distributed and modular computing concepts is shown to facilitate the researcher's selection of component granularity as well as the connectivity and interaction of the simulation components. The case study is specific, however, the techniques employed in addressing the encountered problems are general and applicable to a much broader range of scientific simulation. A paradigm is developed through which the burden of information management in distributed Monte Carlo simulations is lessened through realization of a modular system of agents that may be augmented as a virtual collaborative community.

An understanding of the physics to be simulated is a prerequisite of model development. Research has been conducted to provide the required understanding of the associated knowledge domain. The separable nature of the processes involved in air fluorescence provide suitable processes for a modular distributed simulation. Physical processes that can be decoupled and implemented as modular physics agents have been identified.

Models suitable for decoupling are implemented as OSGi bundles used by JADE agents. The OSGi architecture is used to define the types of data consumed and produced by models of a given physical process with no concern of specific implementation of the model. This allows third party developers freedom to implement models to their required level of detail with only the restriction of the model's input and output upholding the contract defined by the framework. Agents for simulation of physical processes are based on published physics models and experimental data identified by a literature search. Agents simulating random processes employ a statistical technique known as the Monte Carlo Method.

The significance of this work extends beyond demonstrating the new paradigm for agency-oreinted Monte Carlo simulation that is both modular and extensible. The production of air fluorescence via interactions of ionizing radiation with atmospheric gases is a subject ongoing research. Development of Monte Carlo simulation of electron impact induced air fluorescence is of considerable value to related research efforts. Therefore, an opportunity exists not only to demonstrate the use of a modular agent-based paradigm for Monte Carlo simulation, but also to provide new capabilities for the investigation of physical phenomena.

The University of Southern Mississippi

# MONTE CARLO SIMULATION OF ELECTRON-INDUCED AIR FLUORESCENCE UTILIZING MOBILE AGENTS: A NEW PARADIGM FOR COLLABORATIVE SCIENTIFIC SIMULATION

by

Christopher Daniel Walker

A Dissertation
Submitted to the Graduate School
of The University of Southern Mississippi
in Partial Fulfillment of the Requirements
for the Degree of Doctor of Philosophy

Approved:

Dia Ali
Director

Ray Seyfarth

Beddhu Murali

Christopher Winstead

Grayson Rayborn

Susan A. Siltanen
Dean of the Graduate School

August 2011

# TABLE OF CONTENTS

# LIST OF ILLUSTRATIONS

**Figure**

# LIST OF TABLES

**Table**

# LIST OF ABBREVIATIONS

| | |
|---|---|
| **EEDL** | Evaluated Electron Data Library |
| **eV** | electron-volt |
| **GS** | Green Sawada [13] |
| **JG** | Jackman Green [17] |
| **JGG** | Jackman Garvey Green [10] |
| **keV** | kilo-electron-volt (1000 eV) |
| **MC** | Monte Carlo |
| **MeV** | mega-electron-volt (1000 keV) |
| $\mathbf{N_2}$ | molecular nitrogen |
| $\mathbf{N_2^+}$ | molecular nitrogen ion |
| $\mathbf{O_2}$ | molecular oxygen |
| **OBP** | Opal Beaty Peterson [22] |
| **TSSK** | Tabata Shirau Sataka Kubo [29] |

# Chapter 1

# INTRODUCTION

## 1.1 Overview

Design and development of Monte Carlo simulations for physical systems of moderate complexity can present a seemingly overwhelming endeavor. The researcher must possess or otherwise develop a thorough understanding the physical system, create mathematical and computational models of the physical system's components, and forge a simulation utilizing those models. While there is no single route between a collection of physical concepts and a Monte Carlo simulation based on those concepts, this work develops a new paradigm based on agent-oriented architecture and modular design principles through a case study in which interactions between electrons and molecules are simulated. A methodology that incorporates both distributed and modular computing concepts is shown to facilitate the researcher's selection of component granularity as well as the connectivity and interaction of the simulation components. The case study is specific, however, the techniques employed in addressing the encountered problems are general and applicable to a much broader range of scientific simulation. The result of this work is a paradigm in which the burden of Monte Carlo simulation is lessened through realization of a modular system of agents that may be augmented as a virtual collaborative community.

## 1.2 A New Paradigm

The primary objective of a paradigm is to produce a conceptual approach to problem solving in a particular application domain. It provides a framework in which a practitioner can develop and manage abstract ideas in a meaningful way. The object-oriented paradigm presents computational abstractions as representatives of physical objects, their attributes, and their actions. The agent-oriented paradigm extends the object-orient paradigm by declaring the objects to be actors and their actions to be behaviors. The current work moves farther along that line of thinking by specifying the actors are representations of virtual scientists, their behaviors encapsulate abilities to perform computational tasks related to a specific scientific objective. The objective of the new paradigm is to move agent-based computing beyond the confines of software engineering and into the realm of computing

for physical science. Therefore, much effort has gone into casting the abstractions into forms that are more familiar to the physical scientist. Physical scientists are accustomed to working as teams in which individual capabilities contribute to a specific objective. Multiple teams often collaborate on large projects and the capabilities of individual scientists are aggregated into team capabilities. Rather than focusing on the agent, the current paradigm expands upon concept of the agency to form a new agency-oriented paradigm for scientific computing.

Tveit [30] notes that the adoption of a new paradigm requires development of "robust and easy-to-use methodologies and tools." Much of the work in support of the new paradigm's proof of concept involved exploring methods for increasing the agility of an agent based system while minimizing the burden of the user. In general, the agency has previously been seen as the application that hosts computational agents. The new way of thinking presents it as much more. The agency should now be viewed as a tool that assists scientists in development, deployment, and management of a community of agents and modular artifacts representing scientific capabilities. Furthermore, an overall system of agencies is envisioned as a community of virtual scientists cooperating to achieve a simulated scientific objective.

## 1.3 Thesis Structure

The introductory chapter provides a high level view of the work and detailed treatment of the individual components is left to subsequent chapters. By the end of this chapter, the reader should be familiar with the general concept of the work, the chosen case study, and the initial high level problems to be addressed.

Chapter 2 reviews the available literature. In section 2.1 an overview of the references related to the analytic modeling of interaction cross sections and the associated reference data is provided. The history of Monte Carlo simulation is reviewed in section 2.2. Modularity and multi-agent frameworks are reviewed in sections 2.3 and 2.4.

Chapter 3 provides an introductory overview of electron impact induced air fluorescence, the processes involved, and the rational for its utilization as the subject of a case study for modular, agent-based, Monte Carlo simulation.

Chapter 4 dives deep into the analytic models and reference data for the elastic scattering of electrons by molecular nitrogen. Analytic models from both Jackman and Tabata are shown to be in good agreement with the reference data of Itikawa at energies less than 1000 electron-volts and approximately twice the atomic cross section values obtained from Perkins at energies above 1000 electron volts. The consistency between the forms provided by Jackman and Tabata are of importance because the Tabata forms will be used to determine

the probability the occurrence of an elastic scattering event while the Jackman forms will be employed to determine the consequences of an elastic scattering event. Finally, Jackman's analytic form for differential elastic scattering of electrons by molecular nitrogen is shown to be consistent with both his analytic form for total elastic scattering of electrons by molecular nitrogen and the reference data from Shyn.

Chapter 5 examines the analytic models provided by Tabata for the excitation cross sections of molecular nitrogen for electron impact. The comparison of the generated cross sections and experimental data of Majeed as shown by Tabata are recreated here.

Chapter 6 examines the analytic model provided by Tabata for the total ionization cross section and the semi-empirical forms of Jackman et al. for the excitation states of the ionized molecule.

Chapter 7 reviews the analytic form of Tabata et al. for the total electron impact cross section of a nitrogen molecule.

Chapter 8 describes the components utilized in the construction of an agency.

Chapter 9 describes the core modules; components that provide resources for agents but are not agents.

Chapter 10 describes the development of a set of agents employing the previously discussed physics for the simulation of electron interactions with molecular nitrogen at low energies.

Chapter 11 describes an agent developed to coordinate the previously described agents in a Monte Carlo simulation of an interaction that occurs between an electron and a nitrogen molecule. This simulation is responsible for choosing the type of interaction and effecting any consequences of the interaction.

Chapter 12 describes agents that leverage the ability of the agent described in Chapter 11 to carry out a Monte Carlo simulation of an electron cascade in $N_2$ at atmospheric equivalent pressure. The agent described in Chapter 12 first obtains the total $N_2$ cross section from the total cross section agent described in Chapter 10 and use the acquired value in a Monte Carlo selection of distance to the next collision. It then updates the position of the electron and passes the electron to the interaction simulation agent from Chapter 11. That agent simulates the interaction and returns the updated electron to the main simulation agent along with any generated secondary electrons. The main simulation agent repeats this process for each electron until the electron energy is less than the minimum amount required for inelastic interaction with molecular nitrogen. The main simulation agent then reports the results of the simulation to the user. The result depends on the configuration of the main simulation agent but may contain the total number of electrons generated, the number of occurrences of particular interactions, distance traveled by an electron, or an electron's final

position.

Chapter 12 also presents some results of simulation agents developed as part of the case study. Those results are compared to accepted values found in the literature. Quantities chosen as metrics for this work are the mean energy per ionization event, the mean track length of an electron, and the number of excitations to the $C^3\Pi_u$ state per 1MeV primary electron. All of these results are shown to be in reasonable agreement with the accepted standards.

The focus of this work is the low energy interaction of electrons and molecular nitrogen. Chapter 13 concludes the report of the current effort by providing a look forward to continuing and future work that moves beyond molecular nitrogen. Preliminary work for the inclusion of molecular oxygen has been conducted and efforts its integration into an agency system is underway. Through development of extensions to the case study, the paradigm can be tested in larger and more complex scenarios.

## 1.4 A System of Models

Physics contains a system of models that describe or predict the behaviors of physical systems. Those models provide a set of tools from which a scientist may choose depending on the given application's required level of detail. The bulk of a typical introductory college physics text is devoted to the development of a set of basic models describing an object's location and motion. The models provided at the introductory level are often only applicable to simple physical systems or specific system configurations. In classical mechanics, those models are extended or replaced by more sophisticated models to handle more complex and general physical systems. However, the term "classical" foreshadows the fact that these more sophisticated models are themselves only approximations applicable to a limited subset of the possible physical system configurations. The different branches of physics improve the models for the problems specific to their knowledge domain. Statistical physics leverages the power of statistics in modeling the average behavior of physical systems comprising a large number of possible particles or states. Quantum and relativistic physics provide models for systems that are either smaller or move faster than human perception, and consequently behave completely differently than anything in human experience. There are many branches of physics with their own refined models but they are all parts of a system of modular, extensible models.

A theorist constructs mathematical models that predict behaviors of physical systems. An experimentalist constructs physical systems and observes their behaviors. Physics is model centric dialogue between theorists and experimentalists: theorists produce models

that explain or predict physical observations and experimentalists construct systems to test the predictions made by model theory. In practice, the experimentalists make series of observations and infer stochastic behaviors of a physical system. Theorists may automate the evaluation of mathematical models by implementing the models as computer codes. The Monte Carlo method is a computational technique by which computer codes predict stochastic behaviors of systems via evaluation of models using pseudo-random parameters.

The concept of physics building upon itself seems to have recessed in the computational physics branch. Software developed for computational physics is often designed for a specific knowledge domain with no mechanism for extension or interfacing with other computational physics software. For instance, a research scientist may have a tool that simulates a physical process that emits optical photons and another tool that can simulate the transport of optical photon through a physical system but no means of coupling the tools to simulate the transport of optical photons emitted by the process of interest. Another example case involves a researcher that has a tool whose model is too simple for the selected application and although the researcher knows how to appropriately extend the physics, the software provides no extension point for its model.

A higher level of abstraction is needed. This higher level of abstraction should not be only concerned with the modeling of a physical system's behavior, but modeling the physicist as well. A physicist has a set of models applicable for a particular knowledge domain and is capable of extending existing models and acquiring new models. While some physicists are known to work in isolation and hoard their work, the work of a good physicist should be published and consumed by other physicists. These are the behaviors good computational software should emulate: provide a set of models for a specific knowledge domain, mechanisms for extending or replacing models, and mechanisms for communicating with other "virtual physicists." If the software described in the above examples had these capabilities, the results from the simulation of a system producing optical photons could be published and consumed by the software that provides simulation of optical photon transport.

## 1.5 Agent-Based Computing

Braun et al. define a software agent as a software entity that continuously performs tasks given by a user within a particular restricted environment [8]. They provide four features of an agent: autonomy, social behavior, reactivity, and pro-activity. Agents should operate autonomously to complete a user supplied task, communicate with other agents and users, react to events in their environment, and have some mechanism for active planning. These

are the same features we have found desirable for our “virtual physicists.”

## 1.6 Objective

The objective of this work can be summarized as follows: Identify common problems in the design and development of particle-matter interaction simulations that can be decoupled from the specific implementation and provide a reference implementation in such a manner the specific solution may be reused or replaced by third party collaborators. The identification of underlying problems is accomplished via the afore mentioned case study and the desired modularity is achieved through utilization of computational agent and modular frameworks.

## 1.7 Significance of the Research

The significance of this work is two fold. First, it demonstrates a paradigm for agent based Monte Carlo simulation that is both modular and extensible. Second,the production of air fluorescence via interactions of ionizing radiation with atmospheric gases is a subject ongoing research. Development of Monte Carlo simulation of electron impact induced air fluorescence would be of considerable value to related research efforts. Therefore, an opportunity exists to not only demonstrate the use of a modular agent-based paradigm for Monte Carlo simulation, but also provide new capabilities for the investigation of physical phenomena.

## 1.8 Knowledge Domain

The extent of the physics knowledge domain is such that it impossible for an individual’s complete mastery. An attempt to simulate all of physics is far beyond the scope of this work. Rather, implementations for specific subsets physics are provided as a demonstration of the technique. The physical phenomena selected for simulation is interaction of low energy electrons with air, specifically the generation of air fluorescence.

## 1.9 Air Fluorescence

Fluorescence emissions occur in air around high voltage arcs that include natural phenomena such as lightning as well as various man-made electrical systems. Cosmic ray cascades can be detected through the fluorescence they create in the atmosphere. Air fluorescence can also be induced by molecular and atomic interactions involving particles such as energetic photons, electrons, and ions. All of these phenomena result in air fluorescence because they

set into motion a chains of events that result in the production of low energy electrons that excite atmospheric molecules.

## 1.10 Methodology

An understanding of the physics to be simulated is a prerequisite of model development. Research has been conducted to provide the required understanding of the associated knowledge domain. The separable nature of the processes involved in air fluorescence provide suitable processes for a modular distributed simulation.

Physical processes that can be decoupled and implemented as modular physics agents have been identified. Models suitable for decoupling are implemented as OSGi bundles used by JADE agents. The OSGi architecture is used to define the types of data consumed and produced by models of a given physical process with no concern of specific implementation of the model. This allows third party developers freedom to implement models to their required level of detail with only the restriction of the model's input and output upholding the contract defined by the framework.

Agents for simulation of physical processes are based on published physics models and experimental data identified during the literature search. In some cases agents have multiple models and choose the best model according to a criteria. The chosen phenomena also involves random processes. Agents simulating random processes employ a statistical technique known as the Monte Carlo Method.

## 1.11 The Monte Carlo Method

Inference of a system's general behavior through statistical analysis of a large number of observations has long been a technique employed by experimentalists and is a core component of the scientific method. For theorists, applying these techniques in the modeling non-trivial systems was prohibitively labor intensive before the advent of automated computation machines. These statistical techniques became applicable for more complicated systems only after the invention of computational hardware. This use of computational hardware for the generation of theoretical observables and their statistical analysis heralded the birth of computer simulation and a technique that would be known as the Monte Carlo Method.

## 1.12 Monte Carlo Electron Transport Simulator

A Monte Carlo electron transport simulator is a stochastic computational tool for modeling and predicting the average behavior of an electron as it moves through an environment of

interest. In principle, the simulator consists of a model for an environment, a model for the electron, and a model for each of the possible interactions between the electron and the environment. The model environment encapsulates the geometry of the environment of interest and the properties of any medium it contains. The electron model has three primary attributes: position, direction, and energy. Position and direction are given in terms of the environment model geometry, requiring mechanisms for locating the electron as it traverses and interacts with the environment. Interactions modify the direction and energy of the electron, create secondary particles, and modify the medium of the environment. For example, an inelastic scattering interaction could result in a change of direction and loss of energy for the electron and the dissociation of the target molecule.

## 1.13 Problem Domain

Dissection of the problem domain begins with examination of the semantics of the stated objective. The phrase "particle-matter interaction simulation" is taken as an initial point of departure into semantical exploration and each morpheme is addressed in reverse order of occurrence: Simulation in the context of this work is taken to mean the collective use of algorithms and data structures in a computational system to model a physical system in an effort to predict some behavior of the represented system. An interaction is an event involving two or more participants of which the effect is a change of value of one or more observables. Matter is generally defined via two properties: having mass and occupying a volume in space. In general, a particle is set of observables associated with a very small volume.

In this work, the electron is chosen as an instance of a particle. The model of the electron has two mutable observables: position and momentum. Physically, the electron carries other observables including mass and charge. While the mechanism of the interactions between electrons and air are due to the Coulomb force resulting from the carried charge, there is no need to explicitly model this observable as part of the electron as it is immutable. Rather, accounting for the fundamental electronic charge is directly addressed in the interaction models.

For the case study, air is selected as the specific type of matter for which electron interactions are simulated. Air is a mixture of substances of which the primary constituents are molecular nitrogen and molecular oxygen. As a simplification, the case study will focus on nitrogen with an equivalent pressure of 1 atmosphere. The number density of air is $2.5 \text{x} 10^{19}$ molecules per cubic centimeter. A sphere bounding the volume of air in which interactions due to a 1MeV primary electron may occur is calculated to be of a radius of

about 4 meters and thus containing some $6.7 \times 10^{27}$ molecules. Given a hypothetical scheme by which all the parameters for a single molecule is mapped to a single byte, more than 7 trillion terabytes of storage would be required. It is obvious an approach in which individual molecules are modeled is infeasible. Rather, a statistical treatment of air must be employed in which a probability field replaces the individual molecules. In this case, the electron can be considered as experiencing free flight between interactions and the details of the interactions can be determined in the simulation via statistical sampling of the probability fields.

Having explored the particle and matter used in the case study, attention is now turned to the possible interactions. For the purposes of the case study, electron energies up to 1MeV are considered. At these energies, there are three interactions that may occur between electrons and air: elastic scatter, excitation, and ionization.

## 1.14 Summary

In this chapter, a general synopsis of the overall thesis structure was presented along with related supporting introductory material. Physical concepts were framed in terms of a system of models and computational agents were described as having characteristics desired in simulation modules. Distributed and modular computing concepts in Monte Carlo simulations were used to describe a new paradigm that facilitates the researcher's selection of component granularity as well as the connectivity and interaction of simulation components via a community of modular simulations working in collaboration to carry out a larger overall simulation. These communities are made up of agents that encapsulate specific expert knowledge domains and contribute a particular functionality to the agency's ability to perform a simulation task. A case study, the simulation of electron impact air fluorescence was selected as a representative of a scientific simulation project.

# Chapter 2

# AIR FLUORESCENCE, MONTE CARLO SIMULATION, MODULAR SOFTWARE, AND COMPUTATIONAL AGENTS

## 2.1 Air Fluorescence

As noted in Chapter 1, construction of a Monte Carlo simulation for a particular physical system or process requires extensive knowledge of the system or process. For the case study developed in this work, the literature was reviewed in search of appropriate models and data for use in simulating interactions of low energy electrons with the the dominate molecular species found in air: $N_2$. Much related work, both theoretical and experimental, was conducted in aurora and day glow studies in the 1970s. A resurgence of related work occurred in the last decade of the twentieth century when astronomers carried out a series of large experiments for cosmic ray detection. Part of the ongoing work in the cosmic ray community are efforts to consolidate knowledge from prior work. In 2006, Itikawa published a set of reference cross sections for electron interaction with molecular nitrogen based on more than a hundred prior works [15]. Tabata et al. conducted a survey of available data, revisited the analytical cross section forms of Green and McNeal, and in 2006 published 75 recommended analytical models for cross sections of processes related to electron interactions with molecular nitrogen [29]. While these works are substantial, they are not comprehensive. The recommended data of Itikawa does not cover the full energy spectrum of interest in the case study and the recommended analytical models from Tabata do not include cross section models required for determining the deflection angles of scattered electrons, the energy spectrum of secondary electrons ejected in ionization events, or the preferred direction of those secondary electrons. Additional models and data identified by Lee [18] are shown to be compatible with the Tabata et al. models. Analytic models for differential elastic scattering cross sections are found in the work of Jackman and Green [17] and compared to the data from Itikawa [15], Shyn [27], and Perkins [23] as suggested by Lee [18]. Analytic cross section models for the individual ionization states are found in the work of Jackman, Garvey, and Green [10] based on the work of Green and Sawada [13]. The preferential directions of secondary electrons produced by electron impact ionization of molecular nitrogen can be computed via an analytic form provided by Jackman and Green [17]. Air fluorescences continues to be a subject of interest in the

scientific community, especially in astrophysics where it is used to detect the interaction of high energy cosmic rays with the Earth's atmosphere. Arqueros et al. [4] provide a review of historical advancements in the cosmic ray induced air fluorescence measurement methodologies for the period between 1954 and 2000. Not all works referenced by Arqueros are directly applicable to the current investigation: the focus here is the very low energy electrons that are generated as a consequence of interactions of higher energy particles with the atmosphere. However, of particular interest among these are the works of Bunner [9], Davidson and O'Neil [12] [11], and Itikawa [15]. Since 2000, much has been accomplished in continued work in the study of air fluorescence. In 2002, the First International Workshop on Air Fluorescence was held at the University of Utah. To date, the international community has participated in seven air fluorescence workshops and the eighth is scheduled for later this year. The combination of these workshops, a number of experimental efforts, and continued research has produced a wealth of information within the last decade. New measurements of the fluorescence yield from electron impacts in nitrogen have been made [31] [21] [2]. New results from simulations have been produced [1] [3] [7].

## 2.2 Monte Carlo Simulation

Inference of a system's general behavior through statistical analysis of a number of observations or measurements is a core component of the scientific method. This has long been a technique employed by experimentalist. For theorists, applying these techniques in the modeling of non-trivial systems was prohibitively labor intensive before the advent of automated computation machines. These statistical techniques became applicable for more complicated systems only after the invention of computational hardware. The use of computational hardware for simulation of a large scale dynamic process such as an electron cascade in a gas, the standard technique is Monte Carlo simulation. The technique is closely tied to the foundation of computer science.

## 2.3 Modular Computing

Rellermeyer et al. [24] provide a description of a distribution method for OSGi in which they note "Modular design is a corner stone of software engineering and ... recent years have seen the emergence of module management systems." These module management systems provide dynamic loading and unloading of modules in distributed applications. It is noted that the idea of modular development predates OSGi and Common Object Request Broker Architecture (CORBA) and Distributed Component Object Model (DCOM) are referenced as examples of other modular technologies. However, Rellermeyer et al. [24] show their

implementation of OSGi matches or exceeds the performance of mechanisms such as RMI and UpnP. A major boost was given to the OSGi community when the Eclipse Foundation decided to migrate their flagship product, the Eclipse IDE, to an OSGi architecture. Gruber et al. [14] describe the transition from the Eclipse 2.1 proprietary plug-in architecture to the Eclipse 3.0 OSGi-based plug-in architecture. The relationship between the Eclipse Foundation and the OSGi Alliance is also detailed in chapter one of "OSGi and Equinox: Creating Highly Modular Java Systems" [20]. The result of the interaction of one group dedicated to producing a specification for modular Java systems and another group dedicated to implementing a modular Java framework pushed the OSGi technology to the forefront of modern modular development.

## 2.4 Agent-Based Computing

The introductory chapter of the book by Bellifemine et al. [6] provides an introduction to the JADE platform and it's relationship with agent-oriented programming. The concept of agent oriented programming dates back to the work of Shoham [26] in which it was presented as a new "specialization of object-oriented programming." Since 1993, the concept of agent-based systems has evolved and the JADE framework has emerged from that evolution. Among the core concepts of agent-orient programming is the idea that agent-based system includes the ability for autonomous interaction of components for the achievement of a particular goal.

# Chapter 3

# ELECTRON IMPACT-INDUCED AIR FLUORESCENCE

## 3.1 Introduction

Chapter one noted that the concepts in physics build upon themselves. There is temptation when writing about electron - molecular interaction to begin by describing the basic particles (electrons, neutrons, and protons), how those particles form atoms, and the ways atoms combine to form molecules. However, doing so would stray from the topic at hand and into other fields such as chemistry. For the purpose of this work, a molecule is a system that can store or emit energy by reconfiguring its electronic structure and an incident electron is a free electron (not part of a molecule) carrying kinetic energy. The different electronic configurations, known as excited states, store energy and there exist numerous ways a molecule can configure its distribution of electrons depending on the complexity of the molecule. The energy differences between configurations occur in clumps called bands where the differences of energy stored in configurations belonging to a particular band are small compared to the energy differences of configurations belonging to different bands. The molecule may transition to a lower energy electronic configuration by emitting excess energy, often in the form of a photon. This work is primarily concerned with the ultra-violet photons emitted when a nitrogen molecule reconfigures from its $C^3\Pi_u$ state to its $B^3\Pi_g$ state.

The electron - molecular interactions involved in air fluorescence production are well documented and their details are available in the literature [25] [1]. The interaction directly responsible for fluorescence is a molecular electronic excitation followed by a radiative de-excitation. The basic idea of excitation is as follows: an electron interacts with a molecule, the molecule absorbs some energy from the electron, the molecule stores the gained energy by reconfiguring the distribution of its electrons and the incident electron continues along a deflected path with reduced energy. At some later time, the molecule may again reconfigure its electron distribution to a lower energy configuration by ejecting the excess energy as a fluorescence photon. Excitation, however, is not the only or even most probable way electrons interact with molecules. Since the molecule is surrounded by its electron cloud, the impinging electron could be simply deflected by their net electric field with no energy exchange. This deflection of an incident electron with no energy loss

is called elastic scattering. The excitation process described above is a form of inelastic scattering but it is not the only form of inelastic scattering. If enough energy is absorbed from an incident electron that the reconfiguration of the molecule's electron configuration results in a previously bound electron gaining sufficient energy to break free from the molecule, the process is called ionization. There is also the process named Bremsstrahlung by which the incident electron is abruptly decelerated and the energy difference is emitted as a photon. The probability of Bremsstrahlung and other processes such as K-shell emission are statistically unlikely for low energy electrons in air at normal pressures. Statistically unlikely processes are omitted from this work and simulations are provided for the three primary interactions: elastic scattering, excitation, and ionization.

## 3.2 Rational for a Modular, Extensible Architecture

The mechanism by which fluorescence photons are emitted is independent of the chain of events leading to the excitation of the emitter. Simulation of the emission of fluorescence from an excited molecule can be decoupled from the larger chain of events and implemented as a simulation module. Multiple physical processes may produce excited molecules leading to fluorescence and simulations for each of those processes may be developed as independent modules. Furthermore, models of a physical process with various levels of detail may be applicable for differing scenarios. A modular system design may specify the types of data consumed and produced by models of a given physical process with no concern of specific implementation inside the agent. This allows developers freedom to implement models to the required level of detail with only the restriction of the agent communication methods upholding the contract defined by the framework. The separable nature of the processes involved in air fluorescence provides suitable processes for a modular simulation framework.

Rather than designing a large monolithic program to simulate the interactions of electrons with molecular nitrogen, this work takes a component based approach. Agents are designed to exhibit a particular skill and multiple agents work in cooperation to accomplish the overall objective. For instance a particular agent may be designed to choose the appropriate model for calculating the elastic scattering cross section for nitrogen molecules, carry out the selected calculation, and supply the result to the user or another agent. The agent encapsulates the process and has no need to know how or where the result is ultimately used. Furthermore, if users desire alternate methods not supplied by a particular agent, they are free to use a different agent or supply their own agents.

## 3.3 Summary

This chapter has provided an introductory overview of electron impact induced air fluorescence and foreshadowed some of the concepts that will be addressed in detail in later chapters. Furthermore, the rational for using the processes related to electron impact induced air fluorescence in a case study for the development of a paradigm for modular agent based Monte Carlo simulation was given.

# Chapter 4

# ELASTIC SCATTERING OF ELECTRONS BY MOLECULAR NITROGEN

## 4.1 Introduction

Elastic scattering is the simplest interaction considered in this work for electrons and $N_2$ molecules. The electron experiences a change in direction but does not lose energy to the molecule. According to Jackman [16], the maximum energy loss for an electron elastically scattered by a nitrogen molecule is less than one hundredth of a percent of the electron's kinetic energy. For the purpose of the current work, that loss is considered negligible but may be incorporated in a future model. For this interaction, there are only two questions to answer: What is the probability of this interaction occurring relative to the other possible interactions, and in which direction is the electron scattered?

## 4.2 Total Cross Section

The probability of an interaction occurring is calculated using the related cross sections. There are several methods of obtaining the cross sections including experimental data, theoretical formulas, and empirical fits to experimental data. Jackman [16] and Tabata [29] have provided analytical methods for computing total elastic cross sections for electrons scattering from molecular nitrogen. Itikawa [15] provides a set of recommended values for total elastic cross sections. The data from Itikawa, however, only contains primary electron energies up to 1000 electron volts. The energy range is expanded by augmenting doubled atomic cross sections from Perkins [23]. In this section results from the parameterized analytical methods are compared to the recommended values from Itikawa and the approximation data using EEDL.

Scilab, a numerical computation tool, was employed in the comparison of the analytic function and the suggested cross section values. A Scilab script was written using the parameters and form provided by Jackman to compute total elastic cross section over the range of energies covered by Itikawa's suggested values. The values from Itikawa are entered into the script as pairs of energies and cross sections. The suggested values are overlaid on a plot of the analytic function. The Scilab script is provided in program 1 and

the generated plot is shown in figure 4.1. Similar procedures were followed to produce plots for comparison of Jackman and Perkins (Figure 4.2), Itikawa and Tabata (Figure 4.3), and Tabata and Perkins (Figure 4.4).

The analytic form from Tabata is provided in equation 4.1 and its parameters in Table 4.1. Jackman's form and parameters are provided in the code listed in program 1.

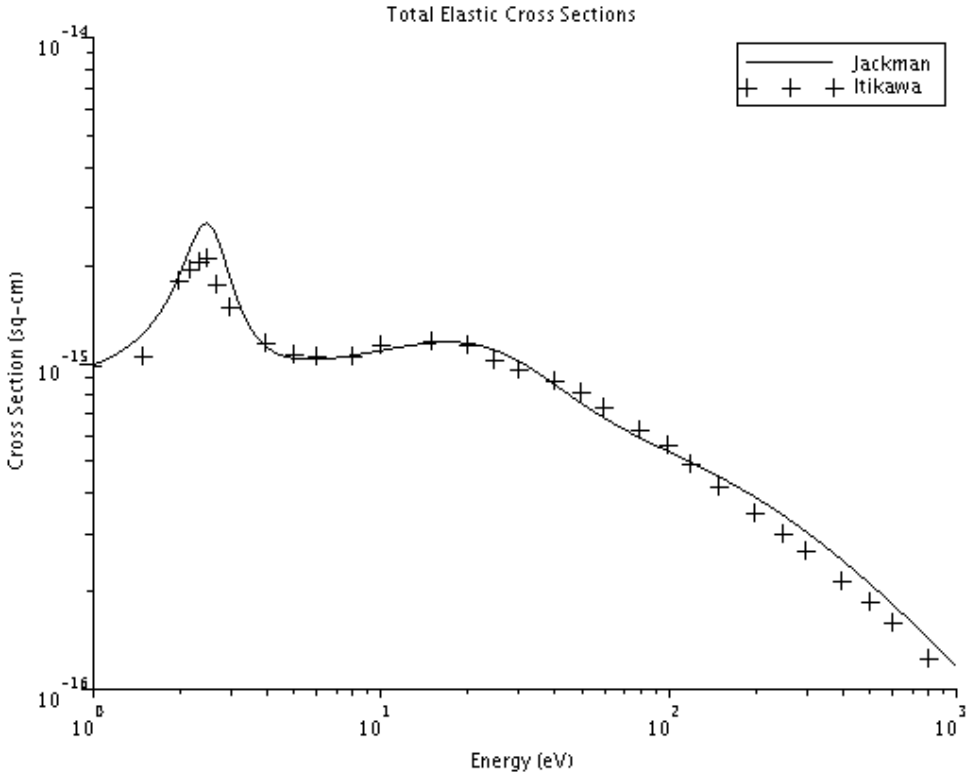


*Figure 4.1*: Total Elastic Cross Sections Of $N_2$ For Electrons (E < 1keV).
A curve generated using an analytic form from Jackman is compared to reference data supplied by Itikawa.

$$\sigma_{elas} = \frac{\sigma_0 c_1 \left(\frac{x}{E_R}\right)^{c_2}}{1 + \left(\frac{x}{c_3} c_2 + c_4\right) + \left(\frac{x}{c_5} c_2 + c_6\right)} + \frac{\sigma_0 c_7 \left(\frac{x}{E_R}\right)^{c_8}}{1 + \left(\frac{x}{c_9} c_8 + c_1 0\right)} \tag{4.1}$$

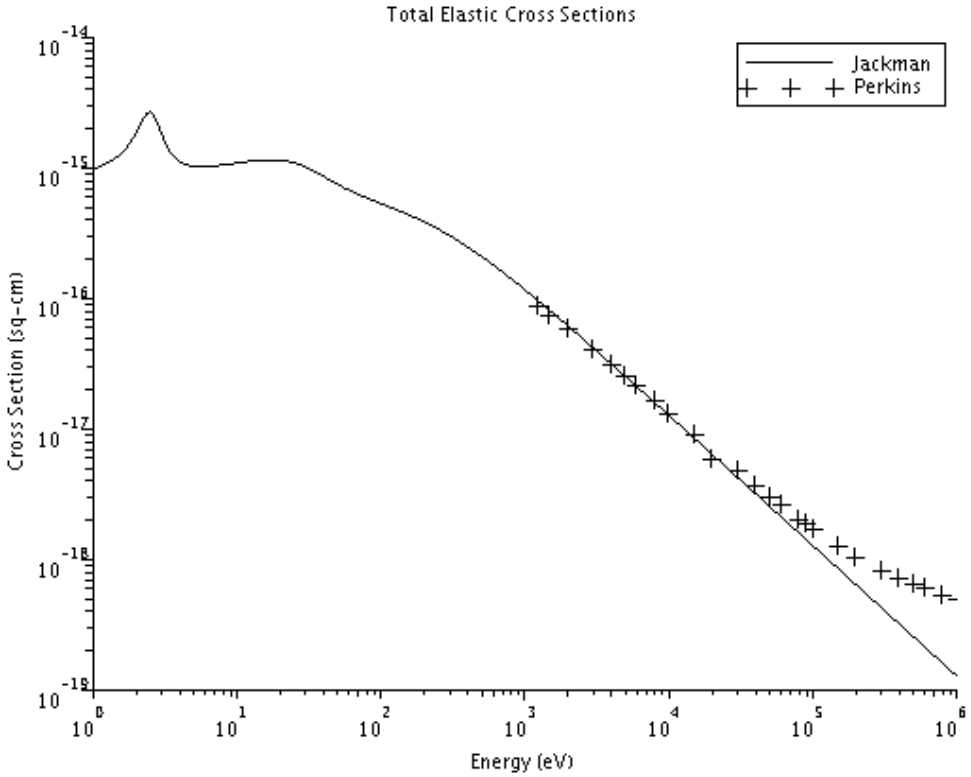


*Figure 4.2*: Total Elastic Cross Sections Of $N_2$ For Electrons (1keV < E < 1MeV)
A curve generate using an analytic form from Jackman is compared to the doubled EEDL atomic cross section data by Perkins.

### 4.3 Differential Cross Section

Differential cross sections are required for computation of the angle by which an elastically scattered electron is deflected. Differential cross sections for elastic scattering are calculated using the technique and parameters suggested by Jackman [16].

$$\frac{d\sigma}{d\Omega} = (T_1 + T_2 + T_3)\sigma \tag{4.2}$$

$$T_1(E,\theta) = -\frac{\left(b(E)^2 - 1\right) f_1(E) e^{\left(-\frac{\theta}{b(E)}\right)}}{2\left(e^{\left(-\frac{\pi}{b(E)}\right)} + 1\right)\pi b(E)^2} \tag{4.3}$$

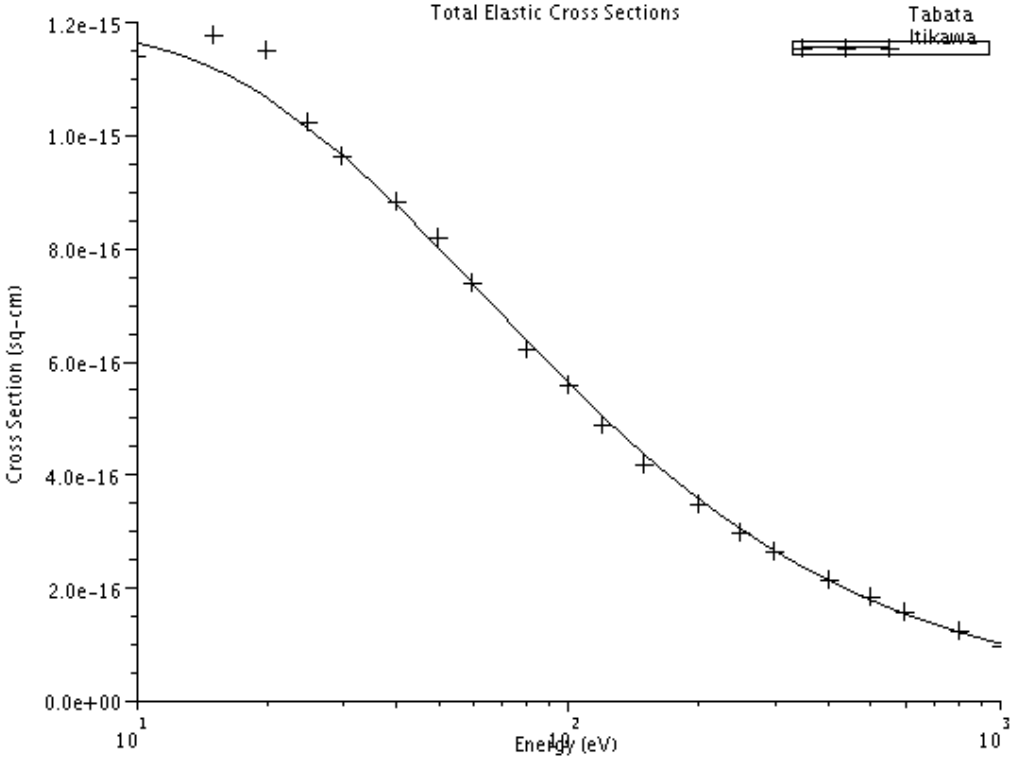


*Figure 4.3*: Total Elastic Cross Sections Of $N_2$ For Electrons (E < 1keV).
A curve generate using an analytic form from Tabata is compared to reference data supplied by Itikawa.

$$T_2(E,\theta) = -\frac{f_2(E)}{2\left(\frac{1}{a+2}-\frac{1}{a}\right)(a-\cos(\theta)+1)^2\pi} \tag{4.4}$$

$$T_3(E,\theta) = \frac{f_1(E)+f_2(E)-1}{2\left(\frac{1}{c(E)+2}-\frac{1}{c(E)}\right)(c(E)+\cos(\theta)+1)^2\pi} \tag{4.5}$$

$$c(E) = -\left(\left(\frac{c_2}{E}\right)^{c_3}-1\right)c_1 \tag{4.6}$$

$$b(E) = E^{b_2}b_1 \tag{4.7}$$

$$f_1(E) = \frac{\left(\frac{E}{f_{11}}\right)^{f_{12}}}{\left(\frac{E}{f_{11}}\right)^{f_{12}}+f_{13}} \tag{4.8}$$

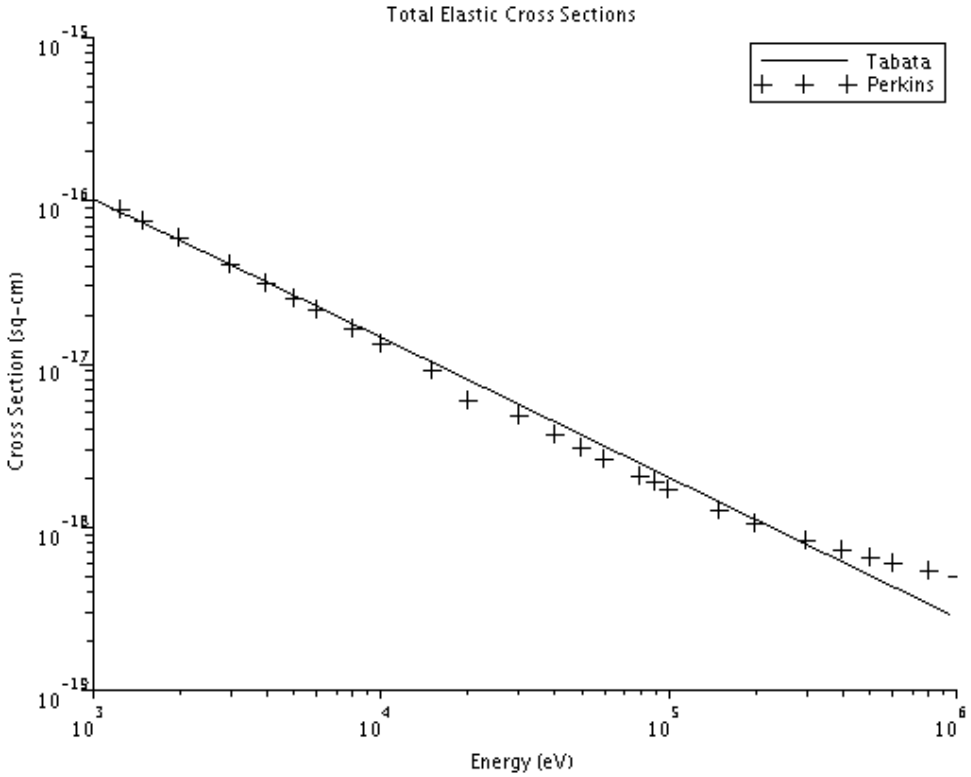


*Figure 4.4*: Total Elastic Cross Sections Of $N_2$ For Electrons (1keV < E < 1MeV).
A curve generate using an analytic form from Tabata is compared to the doubled EEDL atomic cross section data by Perkins.

$$f_2'(E) = \frac{\left(\frac{E}{f_{21}}\right)^{f_{22}}}{\left(\frac{E}{f_{21}}\right)^{f_{22}} + f_{23}} \tag{4.9}$$

$$f_2(E) = \begin{cases} (1 - f_1(E)) f_2'(E) & \text{if } E \leqslant 200eV \\ 1 - f_1(E) & \text{if } E > 200eV \end{cases} \tag{4.10}$$

Values for parameters: $f_{11}$,$f_{12}$ ,$f_{13}$,$a$,$b_1$,$b_2$,$f_{21}$,$f_{22}$,$f_{23}$,$c_1$,$c_2$, and $c_3$ are provided in Table 4.2.

**Program 1** Code containing the analytic elastic scattering cross section form of Jackman

```
//>>>>>>>>>>>>>>>>>>>>>>>>>>>>>>>>>>>>>>>>>>>>>>>>>>>>>>>>>>>>>>>>>>>>>>>>>>>>>>
// Generates a plot for comparison of Jackman's analytical function
// and the suggested N2-e elastic cross section values from Itikawa
//..............................................................

// Parameter list from Jackman
T = 2.5e-16; // Typo in literature gives value as 2.53e-6
U = 1.953e-3;
V = 150.0;
X = -0.77;
G1 = 0.544;
F1 = 7.33;
E1 = 2.47;
G2 = 24.3;
F2 = 2.71;
E2 = 15.5;

// Compute cross section from 1eV to 1KeV
x = 1:0.01:1000;
for(i=1:length(x))
  n = U/x(i);
  y(i) = T*(((x(i)^X)/(n*(n+1)*((V^(2+X))+((x(i)^(2+X)))))+...
  ((F1*G1^2)/((x(i)-E1)^2+(G1^2)))+((F2*G2^2)/((x(i)-E2)^2+(G2^2)))));
end

// Recommended Values via Itikawa
RV = [1.0,9.83; 1.5,10.53; 2.0,17.93; 2.2,19.5;...
2.35,20.5; 2.5,21.0; 2.7,17.5; 3.0,15.0; 4.0,11.6;...
5.0,10.75; 6.0,10.6;8.0,10.6; 10,11.4; 15,11.8;...
20,11.5; 25,10.25; 30,9.65; 40,8.85; 50,8.2; 60,7.4;...
80,6.25; 100,5.6; 120,4.9; 150,4.2; 200,3.5; 250,3.0;...
300,2.65; 400,2.15; 500,1.85; 600,1.6; 800,1.25; 1000,1.0];

plot2d(x,y,logflag='ll')
plot2d(RV(:,1),RV(:,2)*1e-16,style=-1,logflag='ll')
xlabel('Energy (eV)')
ylabel('Cross Section (sq-cm)')
title('Total Elastic Cross Sections')
legend(['Jackman' 'Itikawa'])
//>>>>>>>>>>>>>>>>>>>>>>>>>>>>>>>>> END >>>>>>>>>>>>>>>>>>>>>>>>>>>>>>>>>
```

The differential cross section can be integrated to obtain a total cross section for a selected solid angle and an integration over all space provides the total cross section. The probability of an electron of energy E scattering into a cone defined by $\theta_{cone}$ is the ratio of the integration over the solid angle of the cone to the total cross section.

$$\sigma_{cone}(E,\theta_{cone}) = \int_0^{2\pi}\int_0^{\theta_{cone}} \frac{d\sigma}{d\Omega}\sin\theta d\theta d\phi \tag{4.11}$$

$$\sigma_{total}(E) = \int_0^{2\pi}\int_0^{\pi} \frac{d\sigma}{d\Omega}\sin\theta d\theta d\phi \tag{4.12}$$

*Table 4.1*: Parameters for Equation 4.1.
Parameters used by Tabata [29] in equation 4.1 to generate elastic scattering cross sections of molecular nitrogen for electrons.

| | |
|---|---|
| $a_1$ | $1.440+4$ |
| $a_2$ | $1.284+0$ |
| $a_3$ | $3.190-5$ |
| $a_4$ | $-1.550-1$ |
| $a_5$ | $9.000-4$ |
| $a_6$ | $8.600-1$ |
| $a_7$ | $9.140+5$ |
| $a_8$ | $6.180+0$ |
| $a_9$ | $2.437-3$ |
| $a_{10}$ | $5.980+0$ |

*Table 4.2*: Constants from Jackman [16]

| name | value |
|---|---|
| $f_{11}$ | 100.0 |
| $f_{12}$ | 0.84 |
| $f_{13}$ | 1.92 |
| $a$ | 0.11 |
| $b_1$ | 0.43 |
| $b_2$ | $-0.29$ |
| $f_{21}$ | 10.0 |
| $f_{22}$ | 0.51 |
| $f_{23}$ | 0.87 |
| $c_1$ | 1.27 |
| $c_2$ | 12.0 |
| $c_3$ | 0.27 |

$$P(\theta \leqslant \theta_{cone}) = \frac{\sigma_{cone}}{\sigma_{total}} \tag{4.13}$$

Since the angular dependence is restricted to the phase portion of the cross section, the probability computation may be further simplified.

$$P(E, \theta \leqslant \theta_{cone}) = \frac{\int_0^{2\pi}\int_0^{\theta_{cone}}(T_1+T_2+T_3)\sin\theta d\theta d\phi}{\int_0^{2\pi}\int_0^{\pi}(T_1+T_2+T_3)\sin\theta d\theta d\phi} \tag{4.14}$$

$$P(E,\theta \leqslant \theta_{cone}) = \frac{R_1(E,\theta_{cone}) + R_2(E,\theta_{cone}) + R_3(E,\theta_{cone})}{1 - f_1(E) - \frac{\left(b(E)^2-1\right)\left(\frac{b(E)^2 e^{\left(-\frac{\pi}{b(E)}\right)}}{b(E)^2+1} + \frac{b(E)^2}{b(E)^2+1}\right) f_1(E)}{\left(e^{\left(-\frac{\pi}{b(E)}\right)}+1\right) b(E)^2}} \tag{4.15}$$

$$R_1(E,\theta_{cone}) = \frac{\left(b(E)^2-1\right)\left(\frac{\left(b(E)^2\cos(\theta_{cone}) + b(E)\sin(\theta_{cone})\right)e^{\left(-\frac{\theta_{cone}}{b(E)}\right)}}{b(E)^2+1} - \frac{b(E)^2}{b(E)^2+1}\right) f_1(E)}{\left(e^{\left(-\frac{\pi}{b(E)}\right)}+1\right) b(E)^2} \tag{4.16}$$

$$R_2(E,\theta_{cone}) = \frac{\left(\frac{1}{a-\cos(\theta_{cone})+1} - \frac{1}{a}\right) f_2(E)}{\frac{1}{a+2} - \frac{1}{a}} \tag{4.17}$$

$$R_3(E,\theta_{cone}) = -\frac{\left(\frac{1}{c(E)+2} - \frac{1}{c(E)+\cos(\theta_{cone})+1}\right)\left(f_1(E) + f_2(E) - 1\right)}{\frac{1}{c(E)+2} - \frac{1}{c(E)}} \tag{4.18}$$

The probability of an electron scattering into a region bounded by two cones is the difference of the probability of scattering inside the outer cone and the probability of scattering inside the inner cone.

$$P(\theta|\theta_{inner} \leqslant \theta \leqslant \theta outer) = P(\theta_{outer}) - P(\theta_{inner}) \tag{4.19}$$

The Sage mathematical computing tool was used to evaluate and verify the integrated cross sections forms. The integrated forms were fed back into Sage and evaluated for a range of energies.

Shyn and Carignan [27] have measured the differential cross sections of electrons elastically scattered from nitrogen molecules. The integrated total cross sections are shown to be in agreement with the values calculated following Jackman's approach as illustrated in Figure 4.5. For comparison, the listed Sage program was used to calculate differential cross sections using energies found in Shyn's tables. Differential cross sections were computed for electron energies of 30eV, 100eV, and 400eV. The results, plotted against the values from Shyn [27], are provided in Figure 4.6.

**Program 2** A Sage program for evaluation of scattering cross sections

```
# Parameters from Jackman
f11 = 100.0; f12 = 0.84; f13 = 1.92;
aa = 0.11; b1 = 0.43; b2 = -0.29;
f21 = 10.0; f22 = 0.51; f23 = 0.87;
c1 = 1.27; c2 = 12.0; c3 = 0.27;
TT = 2.5e-16; TU = 1.953e-3; TV = 150;
TX = -0.77; TG1 = 0.544; TF1 = 7.33;
TE1 = 2.47; TG2 = 24.3; TF2 = 2.71;
TE2 = 15.5;

# Jackman's fitting functions
c(E) = c1*(1-((c2/E)^c3))
b(E) = b1*E^b2
f1(E) = ((E/f11)^f12)/(((E/f11)^f12)+f13)
f2P(E) = ((E/f21)^f22)/(((E/f21)^f22)+f23)

def f2(E):
    if E > 200:
        return (1 - f1(E))
    else:
        return f2P(E)*(1 - f1(E))

# Differential phase terms
T1(E,th) = (f1(E)*(1-b(E)^2)*(exp(-th/b(E))))/(2*pi*b(E)^2*(1+exp(-pi/b(E))))
T2(E,th) = -f2(E)/(2*pi*((1/(2+aa))-(1/aa))*((1-cos(th)+aa)^2))
T3(E,th) = ((-1)*(1-f1(E)-f2(E)))/(2*pi*((1/(2+c(E)))-(1/c(E)))*((1+cos(th)+c(E))^2))

# Integrated differential phase terms
I1(E,ti) = f1(E)*(b(E)^2-1)*((((((b(E)^2*cos(ti))+
           (b(E)*sin(ti)))*(exp(-ti/b(E))))/(b(E)^2+1))-
           (b(E)^2/(b(E)^2+1)))/(b(E)^2*(1+(exp(-pi/b(E))))))

I2(E,ti)= (f2(E)*((1/(aa-cos(ti)+1))-(1/aa)))/((1/(aa+2))-(1/aa))

I3(E,ti) = ((-1)*((1/(c(E)+2))+
           (1/(c(E)+cos(ti)+1)))*(f1(E)+f2(E)-1))/((1/(c(E)+2))-
           (1/c(E)))

def SigT(erg):
    TN = TU/erg
    return (TT*(((erg^TX)/(TN*(TN+1)*((TV^(2+TX))+((erg^(2+TX))))))+
    ((TF1*TG1^2)/((erg-TE1)^2+(TG1^2)))+((TF2*TG2^2)/((erg-TE2)^2+(TG2^2))))))

def dSig(erg,tht):
    return (SigT(erg)*(T1(erg,tht)+T2(erg,tht)+T3(erg,tht)))
```

## 4.4 Summary

The analytic models and reference data for the elastic scattering of electrons by molecular nitrogen identified in the literature review have been cross validated for suitability in the

current work. Analytic models from both Jackman and Tabata are shown to be in good agreement with the reference data of Itikawa at energies less than 1000 electron-volts and approximately twice the atomic cross section values obtained from Perkins et al. at energies above 1000 electron volts. The consistency between the forms provided by Jackman and Tabata are of importance because the Tabata forms will be used to determine the probability the occurrence of an elastic scattering event while the Jackman forms will be employed to determine the consequences of an elastic scattering event. Finally, Jackman's analytic form for differential elastic scattering of electrons by molecular nitrogen is shown to be consistent with both his analytic form for total elastic scattering of electrons by molecular nitrogen and the reference data from Shyn.

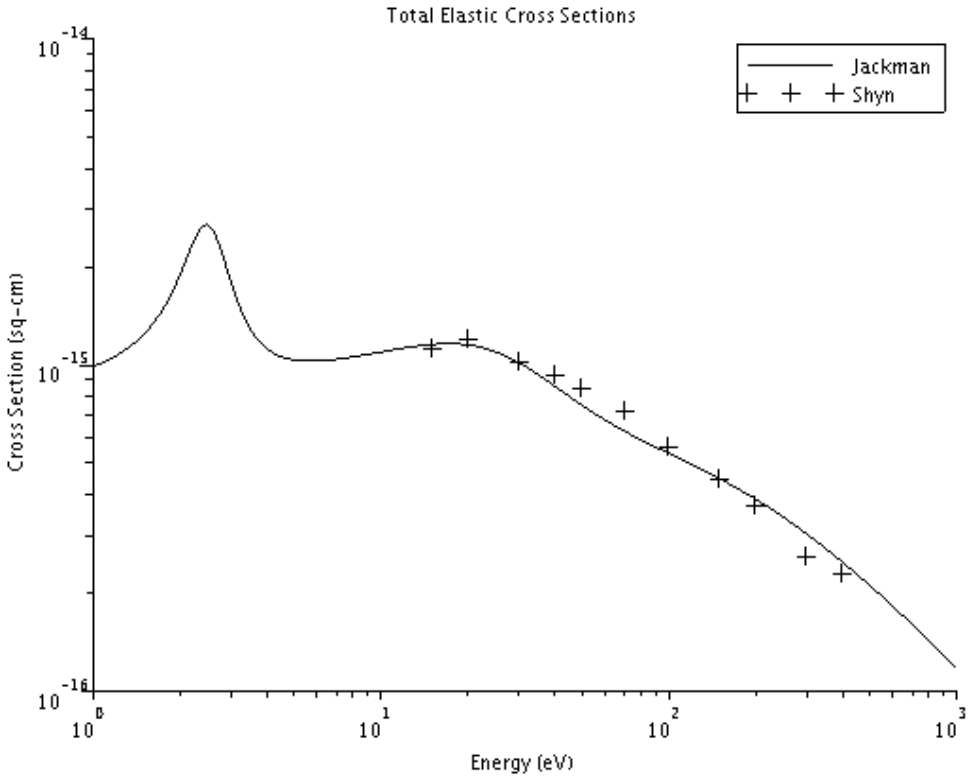


*Figure 4.5*: Summed Differential Elastic Cross Sections.
The differential elastic scattering cross section reference data from Shyn is summed to produce total cross sections and is compared to Jackman's analytic form of total elastic cross sections of molecular nitrogen for an electron

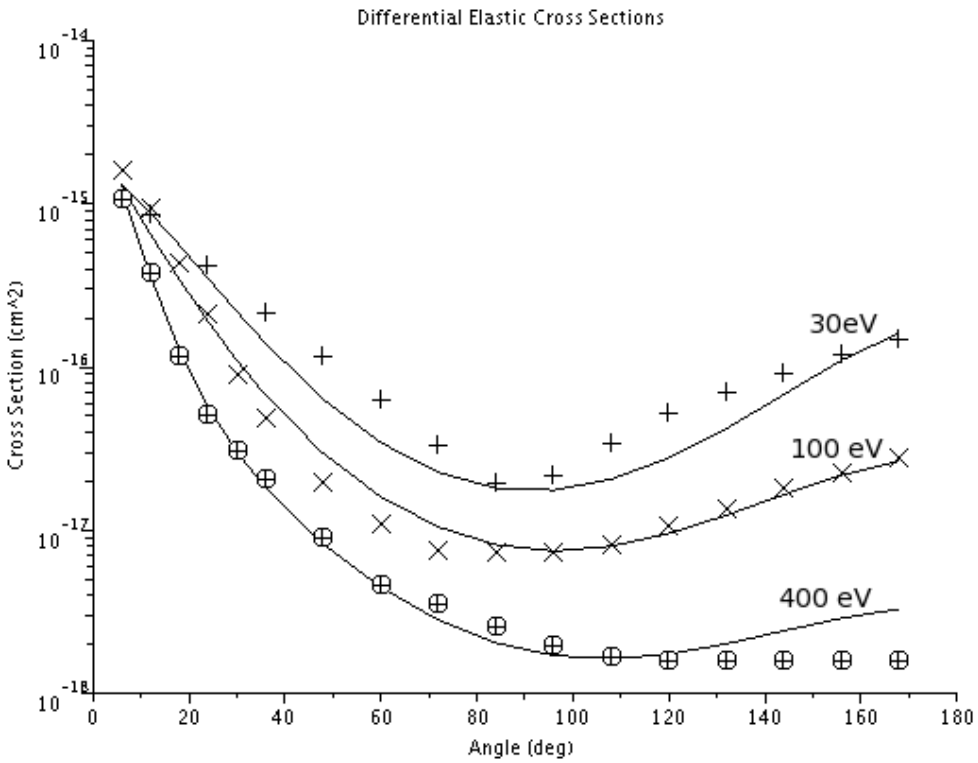


*Figure 4.6*: Differential Elastic Cross Sections.
Jackman's analytic method for differential elastic cross sections is shown in good agreement with Shyn's data.

# Chapter 5

# ELECTRON IMPACT EXCITATION OF MOLECULAR NITROGEN

## 5.1 Introduction

Tabata, Shirai, Sataka, and Kubo [29] have surveyed the available literature and used modified Green-McNeal forms to develop a set of recommended analytic functions for impact cross sections of molecular nitrogen for electrons. In their work, they provided plots of the generated cross sections for comparison with the data identified in their extensive literature search. In this chapter, plots are presented in Figures 5.1 - 5.14 for the cross sections for electron impact excitation of molecular nitrogen in comparison to a subset of the datasets used in Tabata's original work.

## 5.2 The $N_2$ Electron Impact Excitation Cross Sections

In this section plots of cross sections are presented for each of the excitation states of molecular nitrogen along with corresponding analytic form and fit parameters of Tabata et al. [29]. For comparison, each plot presents a subset of the data to which the Tabata et al. forms fit. Much of the data used by Tabata et al. deals with the resonance behavior exhibited at energies lower than is of interest in this work. The data of Majeed and Strickland [19] is the primary source for excitation state cross sections in the energy range of interest.

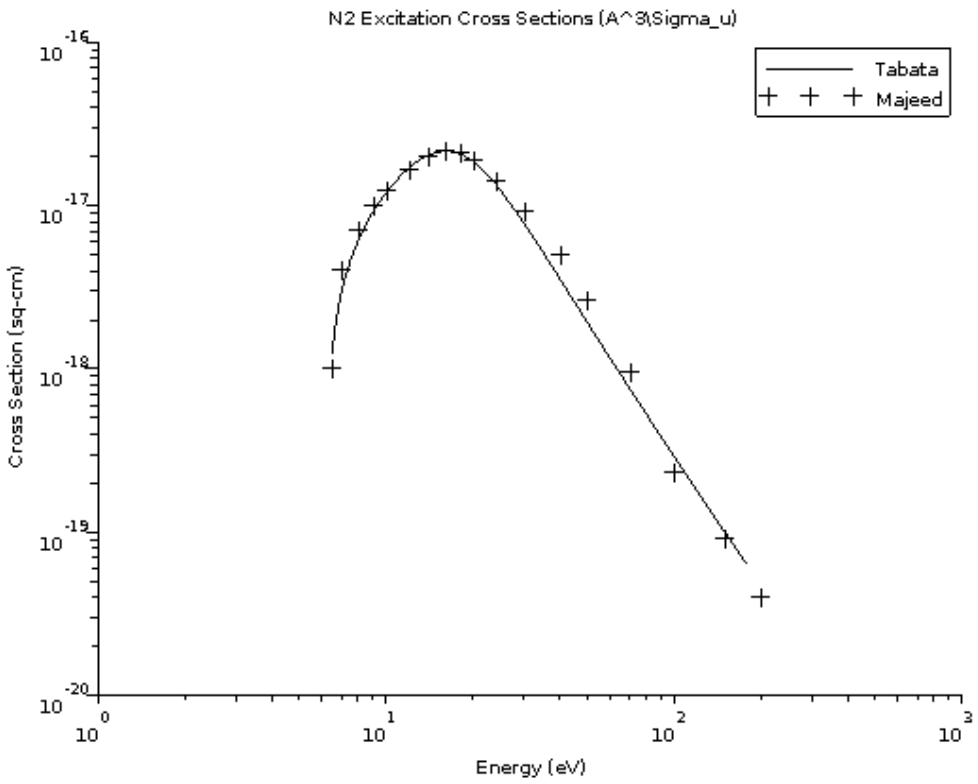


*Figure 5.1*: $A^3\Sigma_u$ Excitation Cross Section.

$$\sigma_{A^3\Sigma_u} = \frac{\sigma_0 c_1 \left(\frac{(E-E_{th})}{E_R}\right)^{c_2}}{1+\left(\frac{(E-E_{th})}{c_3}^{c_2+c_4}\right)} \tag{5.1}$$

*Table 5.1*: Parameters from Tabata [29] for Equation 5.1.

| $E_{th}$ | $c_1$ | $c_2$ | $c_3$ | $c_4$ |
|---|---|---|---|---|
| $6.17E-3$ | $3.97E-1$ | $9.33E-1$ | $1.33E-2$ | $2.503E+0$ |

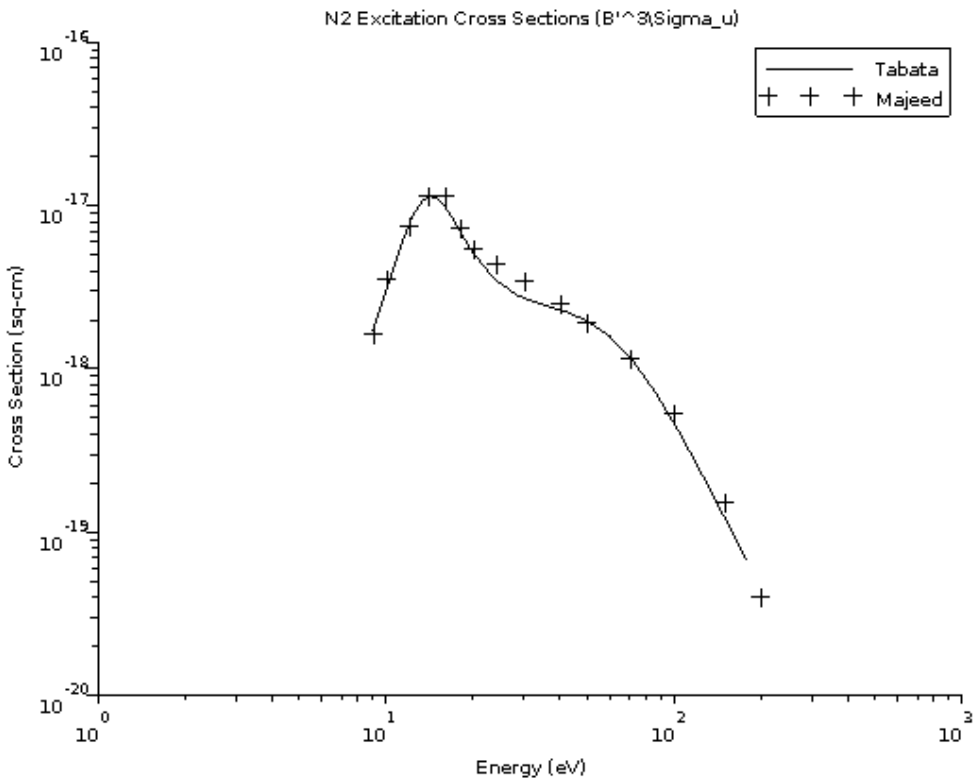


*Figure 5.2*: $B^3\Sigma_u$ Excitation Cross Section.

$$\sigma_{B^3\Sigma_u} = \frac{\sigma_0 c_1 \left(\frac{(E-E_{th})}{E_R}\right)^{c_2}}{1+\left(\frac{(E-E_{th})}{c_3}^{c_2+c_4}\right)} + \frac{\sigma_0 c_5 \left(\frac{(E-E_{th})}{E_R}\right)^{c_6}}{1+\left(\frac{(E-E_{th})}{c_7}^{c_6+c_8}\right)} \tag{5.2}$$

*Table 5.2*: Parameters from Tabata [29] for Equation 5.2.

| $E_{th}$ | $c_1$ | $c_2$ | $c_3$ | $c_4$ |
|---|---|---|---|---|
| $8.16E-3$ | $7.50E-1$ | $1.97E+0$ | $6.70E-3$ | $3.03E+0$ |
| | $c_5$ | $c_6$ | $c_7$ | $c_8$ |
| | $2.12E-2$ | $1.50E-1$ | $5.78E-2$ | $3.39E+0$ |

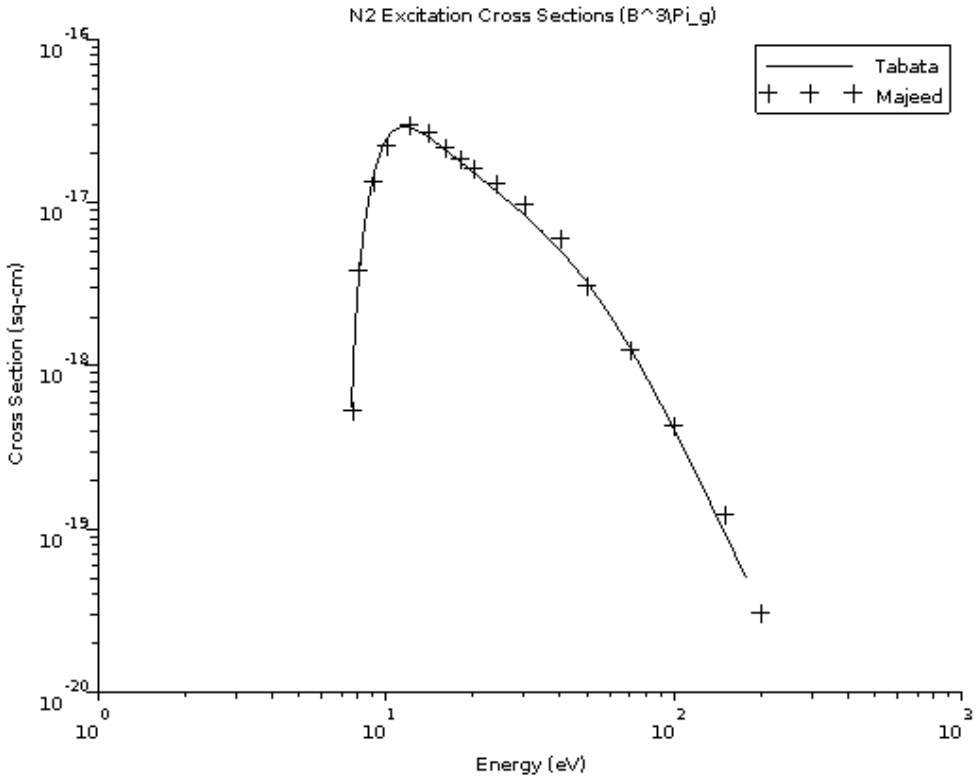


*Figure 5.3*: $B^3\Pi_g$ Excitation Cross Section.

$$\sigma_{B^3\Pi_g} = \frac{\sigma_0 c_1 \left(\frac{(E-E_{th})}{E_R}\right)^{c_2}}{1+\left(\frac{(E-E_{th})}{c_3}^{c_2+c_4}\right)+\left(\frac{(E-E_{th})}{c_5}^{c_2+c_6}\right)} \tag{5.3}$$

*Table 5.3*: Parameters from Tabata [29] for Equation 5.3.

| $E_{th}$ | $c_1$ | $c_2$ | $c_3$ | $c_4$ |
|---|---|---|---|---|
| $7.35E-3$ | $6.82E+0$ | $1.774E+0$ | $3.31E-3$ | $9.15E-1$ |
| | $c_5$ | $c_6$ | | |
| | $1.30E-2$ | $3.65E+0$ | | |

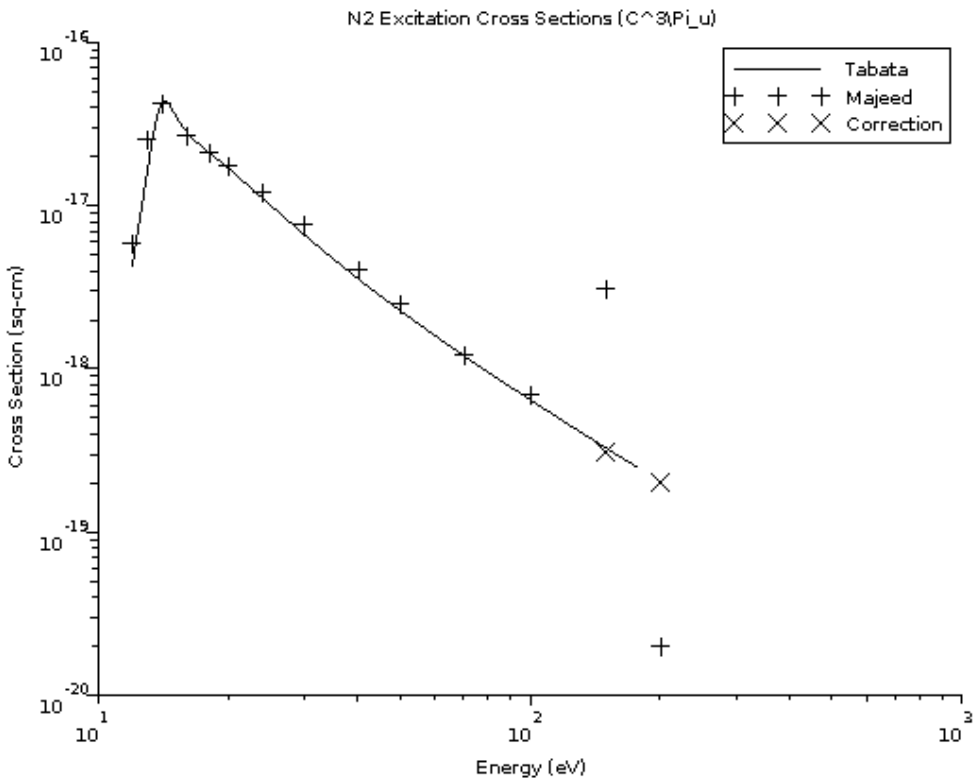


*Figure 5.4*: $C^3\Pi_u$ Excitation Cross Section.

$$\sigma_{C^3\Pi_u} = \frac{\sigma_0 c_1 \left(\frac{(E-E_{th})}{E_R}\right)^{c_2}}{1+\left(\frac{(E-E_{th})}{c_3}^{c_2+c_4}\right)} + \frac{\sigma_0 c_5 \left(\frac{(E-E_{th})}{E_R}\right)^{c_6}}{1+\left(\frac{(E-E_{th})}{c_7}^{c_6+c_8}\right)} \tag{5.4}$$

A correction to an error in the reference tabulation is shown. A typographic error places one too few zeros after the decimal place in the first case and one zero too many in the second case.

*Table 5.4*: Parameters from Tabata [29] for Equation 5.4.

| $E_{th}$ | $c_1$ | $c_2$ | $c_3$ | $c_4$ |
|---|---|---|---|---|
| $1.10E-2$ | $6.82E+2$ | $4.75E+0$ | $3.06E-3$ | $3.62E+0$ |
| | $c_5$ | $c_6$ | $c_7$ | $c_8$ |
| | $1.0E+0$ | $1.212E+0$ | $6.17E-3$ | $1.529E+0$ |

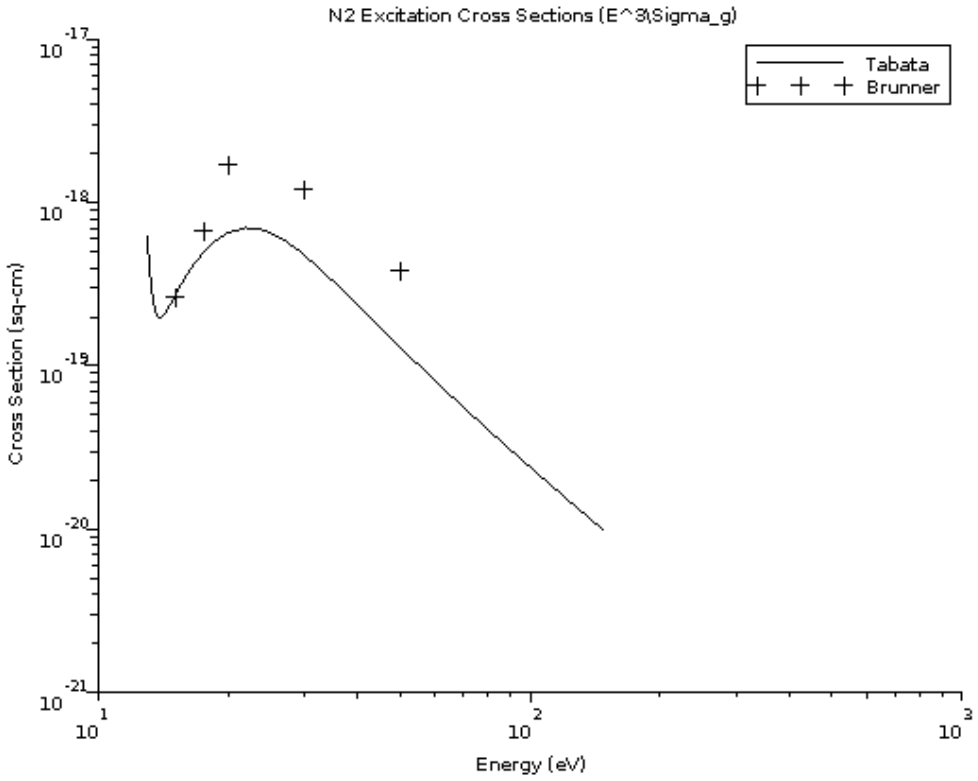


*Figure 5.5*: $E^3\Sigma_u$ Excitation Cross Section.

$$\sigma_{E^3\Sigma_u} = \frac{\sigma_0 c_1 \left(\frac{(E-E_{th})}{E_R}\right)^{c_2}}{1+\left(\frac{(E-E_{th})}{c_3}^{c_2+c_4}\right)} + \frac{\sigma_0 c_5 \left(\frac{(E-E_{th})}{E_R}\right)^{c_6}}{1+\left(\frac{(E-E_{th})}{c_7}^{c_6+c_8}\right)} + \frac{\sigma_0 c_9 \left(\frac{(E-E_{th})}{E_R}\right)^{c_10}}{1+\left(\frac{(E-E_{th})}{c_11}^{c_10+c_12}\right)} \tag{5.5}$$

*Table 5.5*: Parameters from Tabata [29] for Equation 5.5.

| $E_{th}$ | $c_1$ | $c_2$ | $c_3$ | $c_4$ |
|---|---|---|---|---|
| $1.19E-2$ | $1.75E-2$ | $-3.28E-1$ | $3.73E-4$ | $9.55E+0$ |
| | $c_5$ | $c_6$ | $c_7$ | $c_8$ |
| | $7.19E+7$ | $6.75E+0$ | $6.29E-4$ | $4.35E+0$ |
| | $c_9$ | $c_{10}$ | $c_{11}$ | $c_{12}$ |
| | $1.54E-2$ | $1.21E+0$ | $1.23E-2$ | $2.05E+0$ |

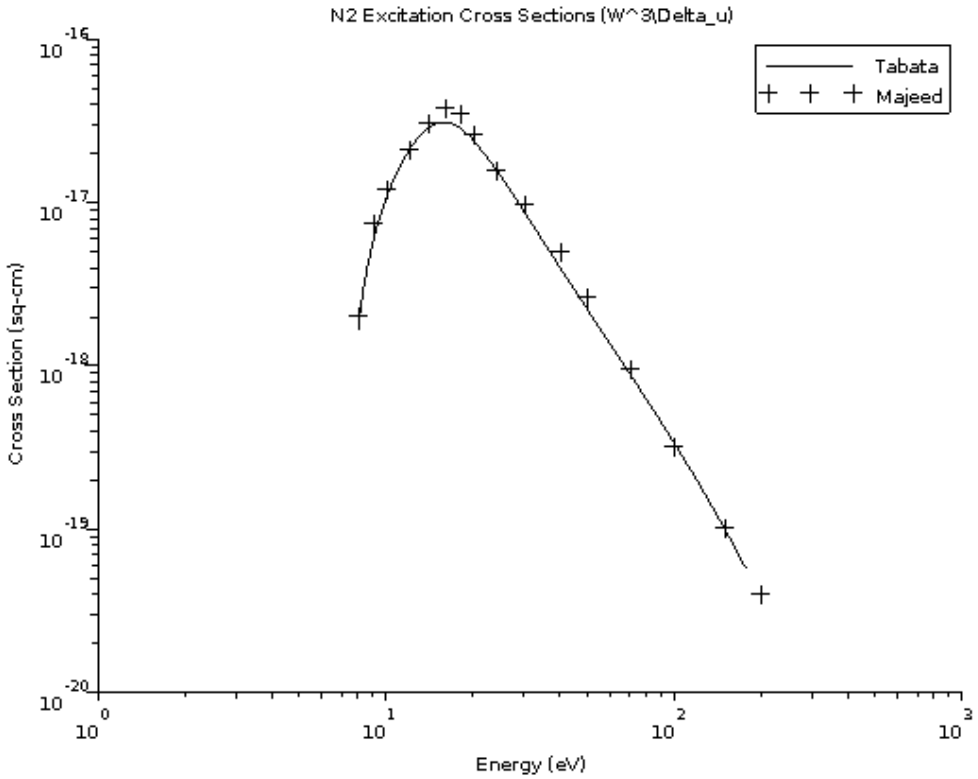


*Figure 5.6*: $W^3\Delta_u$ Excitation Cross Section.

$$\sigma_{W^3\Delta_u} = \frac{\sigma_0 c_1 \left(\frac{(E-E_{th})}{E_R}\right)^{c_2}}{1 + \left(\frac{(E-E_{th})}{c_3}^{c_2+c_4}\right) + \left(\frac{(E-E_{th})}{c_5}^{c_2+c_6}\right)} \tag{5.6}$$

*Table 5.6*: Parameters from Tabata [29] for Equation 5.6.

| $E_{th}$ | $c_1$ | $c_2$ | $c_3$ | $c_4$ |
|---|---|---|---|---|
| $7.36E-3$ | $9.14E-1$ | $1.31E+0$ | $9.90E-3$ | $2.23E+0$ |
| | $c_5$ | $c_6$ | | |
| | $3.10E-2$ | $4.50E+0$ | | |

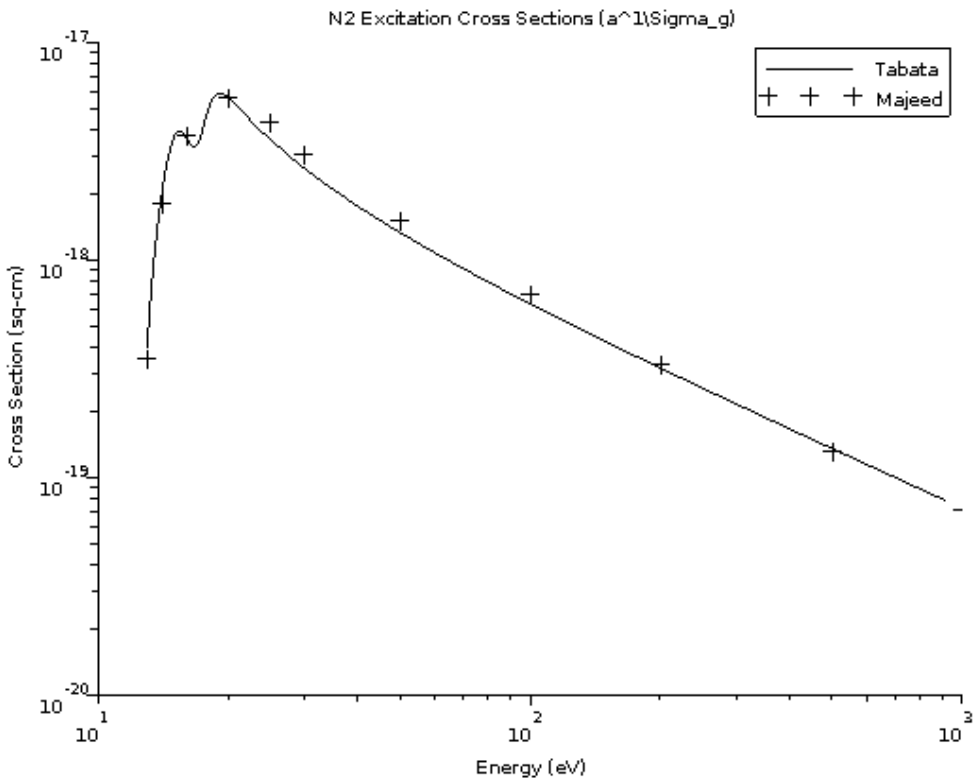


*Figure 5.7*: $a^1\Sigma_g$ Excitation Cross Section.

$$\sigma_{a^1\Sigma_g} = \frac{\sigma_0 c_1 \left(\frac{(E-E_{th})}{E_R}\right)^{c_2}}{1+\left(\frac{(E-E_{th})}{c_3}^{c_2+c_4}\right)} + \frac{\sigma_0 c_5 \left(\frac{(E-E_{th})}{E_R}\right)^{c_6}}{1+\left(\frac{(E-E_{th})}{c_7}^{c_6+c_8}\right)} \tag{5.7}$$

*Table 5.7*: Parameters from Tabata [29] for Equation 5.7.

| $E_{th}$ | $c_1$ | $c_2$ | $c_3$ | $c_4$ |
|---|---|---|---|---|
| $1.23E-2$ | $8.88E-1$ | $1.86E+0$ | $3.56E-3$ | $3.77E+0$ |
| | $c_5$ | $c_6$ | $c_7$ | $c_8$ |
| | $1.14E+2$ | $8.42E+0$ | $5.68E-3$ | $8.93E-1$ |

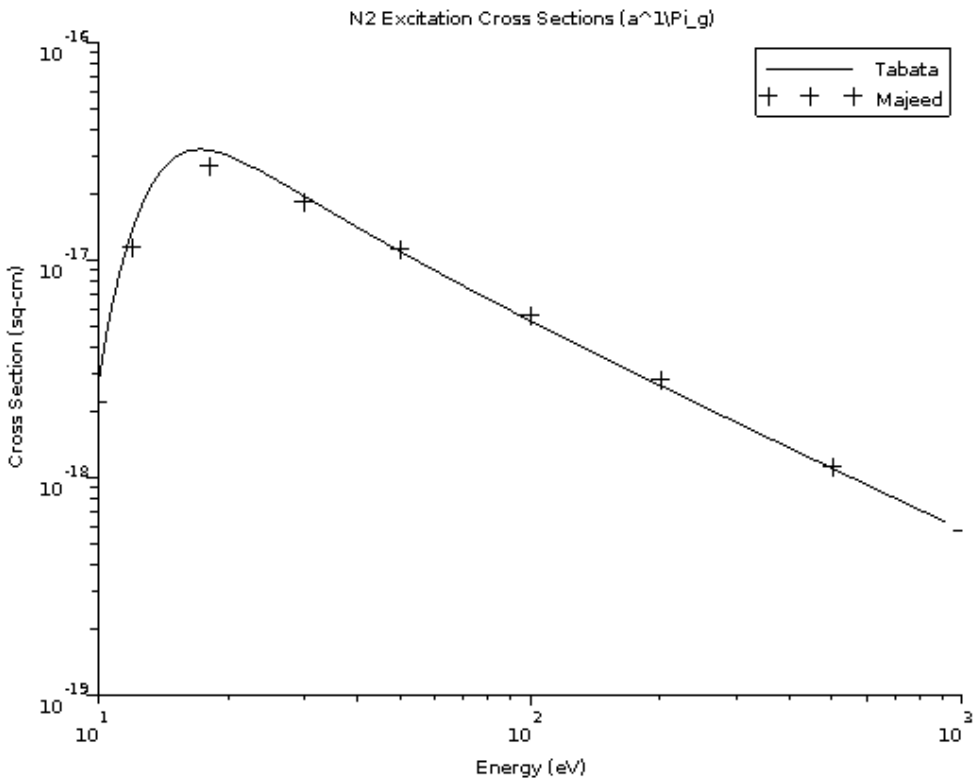


*Figure 5.8*: $a^1\Pi_g$ Excitation Cross Section.

$$\sigma_{a^1\Pi_g} = \frac{\sigma_0 c_1 \left(\frac{(E-E_{th})}{E_R}\right)^{c_2}}{1+\left(\frac{(E-E_{th})}{c_3}^{c_2+c_4}\right)} \tag{5.8}$$

*Table 5.8*: Parameters from Tabata [29] for Equation 5.8.

| $E_{th}$ | $c_1$ | $c_2$ | $c_3$ | $c_4$ |
|---|---|---|---|---|
| $8.55E-4$ | $2.56E+0$ | $2.04E+0$ | $6.69E-3$ | $9.30E-1$ |

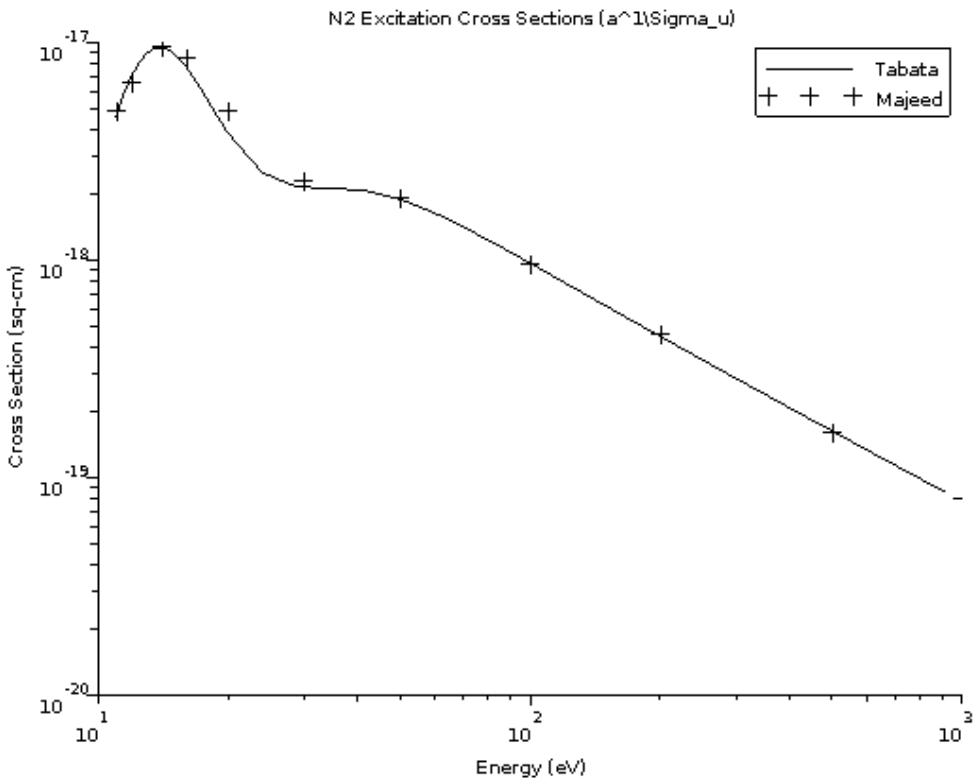


*Figure 5.9*: $a^1\Sigma_u$ Excitation Cross Section.

$$\sigma_{a^1\Sigma_u} = \frac{\sigma_0 c_1 \left(\frac{(E-E_{th})}{E_R}\right)^{c_2}}{1+\left(\frac{(E-E_{th})}{c_3}^{c_2+c_4}\right)} + \frac{\sigma_0 c_5 \left(\frac{(E-E_{th})}{E_R}\right)^{c_6}}{1+\left(\frac{(E-E_{th})}{c_7}^{c_6+c_8}\right)} \tag{5.9}$$

*Table 5.9*: Parameters from Tabata [29] for Equation 5.9.

| $E_{th}$ | $c_1$ | $c_2$ | $c_3$ | $c_4$ |
|---|---|---|---|---|
| $8.40E-3$ | $6.09E-1$ | $1.55E+0$ | $6.23E-3$ | $2.63E+0$ |
| | $c_5$ | $c_6$ | $c_7$ | $c_8$ |
| | $8.26E-3$ | $2.10E+0$ | $2.72E-2$ | $1.061E+0$ |

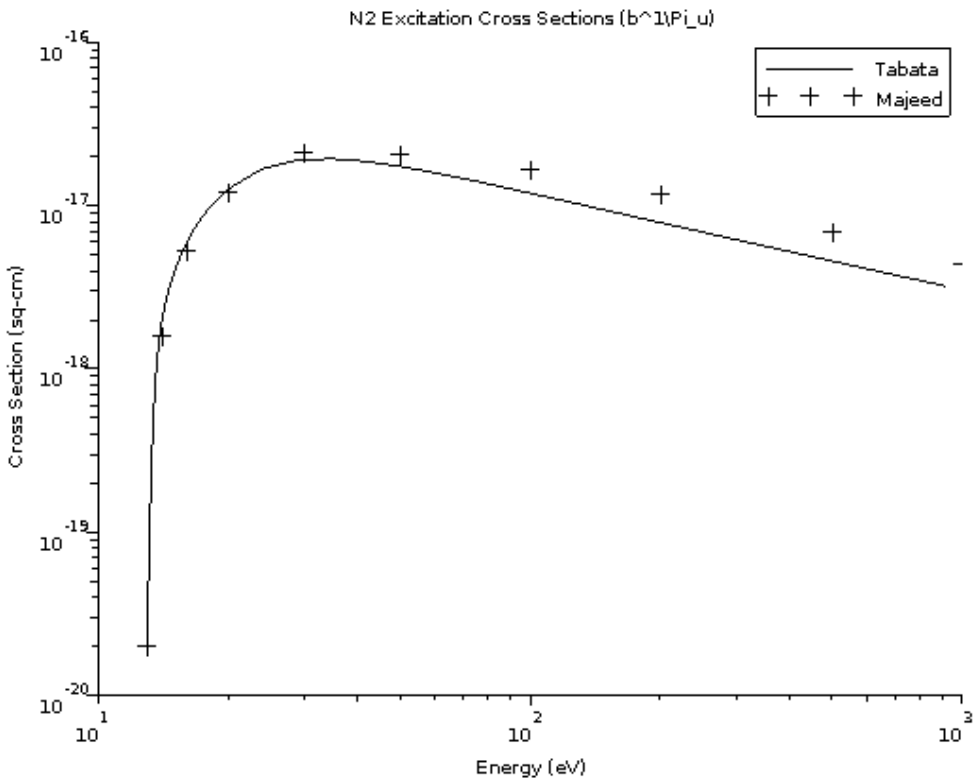


*Figure 5.10*: $b^1\Pi_u$ Excitation Cross Section.

$$\sigma_{b^1\Pi_u} = \frac{\sigma_0 c_1 \left(\frac{(E-E_{th})}{E_R}\right)^{c_2}}{1+\left(\frac{(E-E_{th})}{c_3}^{c_2+c_4}\right)+\left(\frac{(E-E_{th})}{c_5}^{c_2+c_6}\right)} \tag{5.10}$$

*Table 5.10*: Parameters from Tabata [29] for Equation 5.10.

| $E_{th}$ | $c_1$ | $c_2$ | $c_3$ | $c_4$ |
|---|---|---|---|---|
| $1.25E-2$ | $8.91E+4$ | $6.02E+0$ | $9.88E-4$ | $-1.29E+0$ |
| | $c_5$ | $c_6$ | | |
| | $2.07E-3$ | $5.75E-1$ | | |

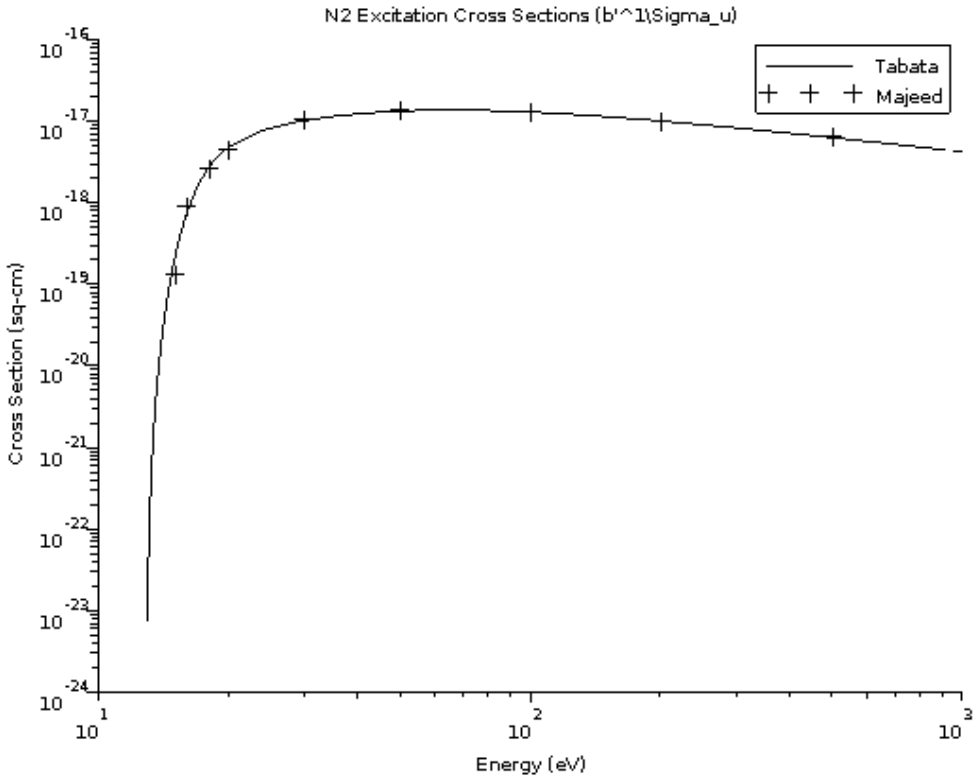


*Figure 5.11*: $b^1\Sigma_u$ Excitation Cross Section.

$$\sigma_{b^1\Sigma_u} = \frac{\sigma_0 c_1 \left(\frac{(E-E_{th})}{E_R}\right)^{c_2}}{1+\left(\frac{(E-E_{th})}{c_3}^{c_2+c_4}\right)+\left(\frac{(E-E_{th})}{c_5}^{c_2+c_6}\right)} \tag{5.11}$$

*Table 5.11*: Parameters from Tabata [29] for Equation 5.11.

| $E_{th}$ | $c_1$ | $c_2$ | $c_3$ | $c_4$ |
|---|---|---|---|---|
| $1.29E-2$ | $2.28E+0$ | $3.80E+0$ | $5.03E-3$ | $-7.70E-1$ |
| | $c_5$ | $c_6$ | | |
| | $9.80E-3$ | $5.90E-1$ | | |

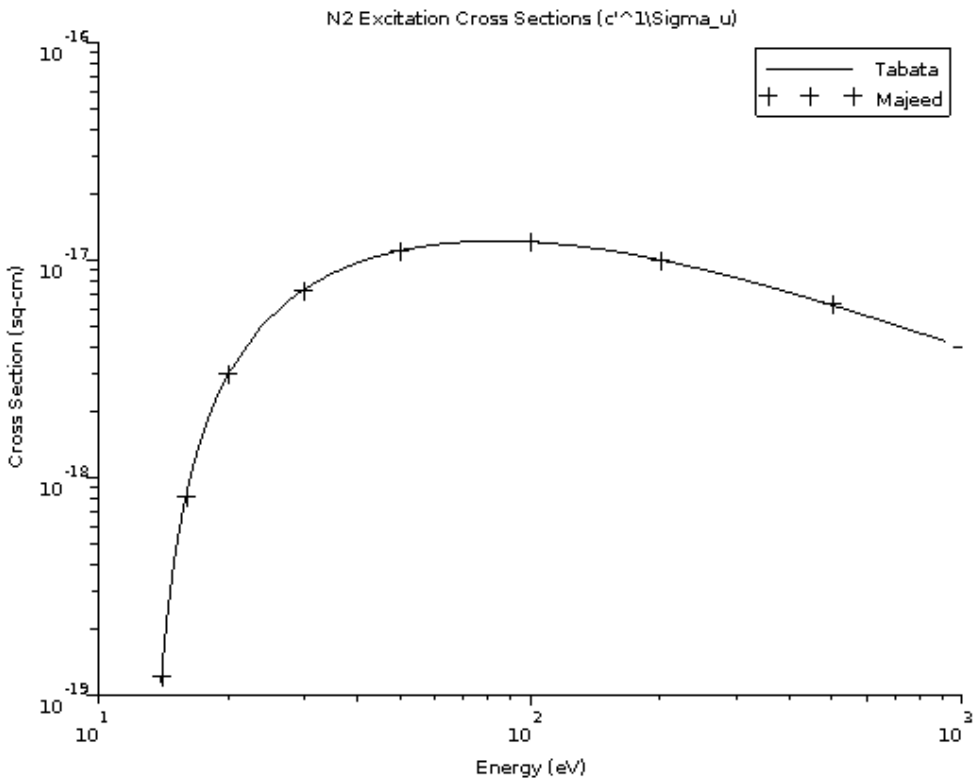


*Figure 5.12*: $c^1\Sigma_u$ Excitation Cross Section.

$$\sigma_{c^1\Sigma_u} = \frac{\sigma_0 c_1 \left(\frac{(E-E_{th})}{E_R}\right)^{c_2}}{1+\left(\frac{(E-E_{th})}{c_3}^{c_2+c_4}\right)+\left(\frac{(E-E_{th})}{c_5}^{c_2+c_6}\right)} \tag{5.12}$$

*Table 5.12*: Parameters from Tabata [29] for Equation 5.12.

| $E_{th}$ | $c_1$ | $c_2$ | $c_3$ | $c_4$ |
|---|---|---|---|---|
| $1.29E-2$ | $2.17E-1$ | $2.04E+0$ | $7.83E-3$ | $-5.55E-1$ |
| | $c_5$ | $c_6$ | | |
| | $2.23E-2$ | $7.02E-1$ | | |

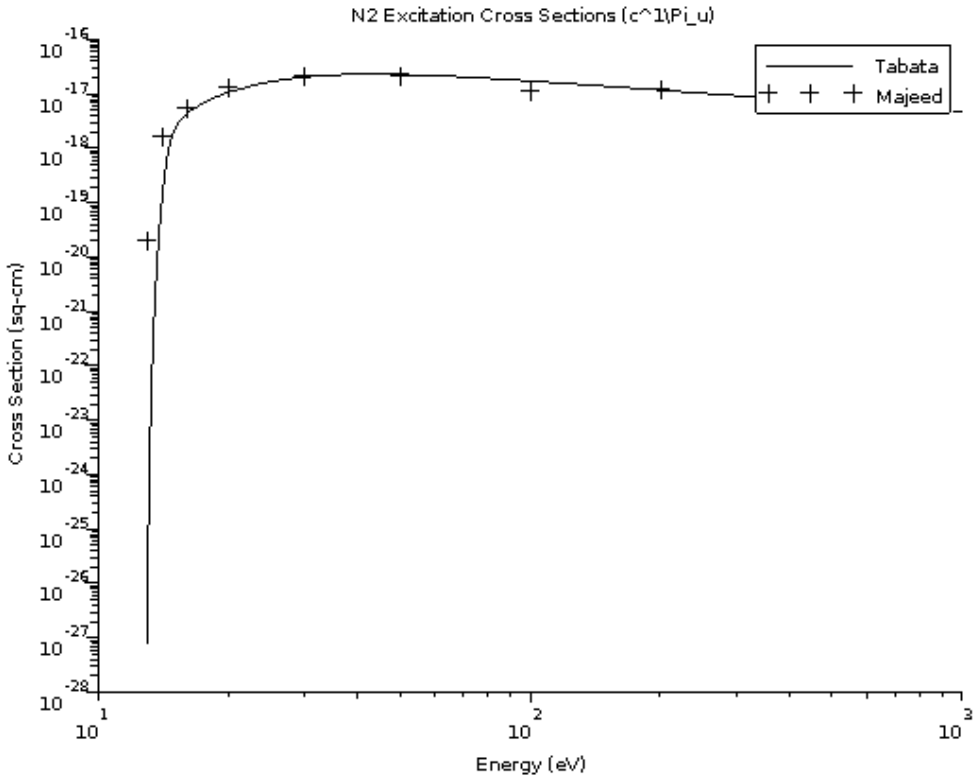


*Figure 5.13*: $c^1\Pi_u$ Excitation Cross Section.

$$\sigma_{c^1\Pi_u} = \frac{\sigma_0 c_1 \left(\frac{(E-E_{th})}{E_R}\right)^{c_2}}{1+\left(\frac{(E-E_{th})}{c_3}^{c_2+c_4}\right)+\left(\frac{(E-E_{th})}{c_5}^{c_2+c_6}\right)} \tag{5.13}$$

*Table 5.13*: Parameters from Tabata [29] for Equation 5.13.

| $E_{th}$ | $c_1$ | $c_2$ | $c_3$ | $c_4$ |
|---|---|---|---|---|
| $1.21E-2$ | $9.02E+4$ | $7.33E+0$ | $1.70E-3$ | $-1.23E+0$ |
| | $c_5$ | $c_6$ | | |
| | $2.97E-3$ | $5.72E-1$ | | |

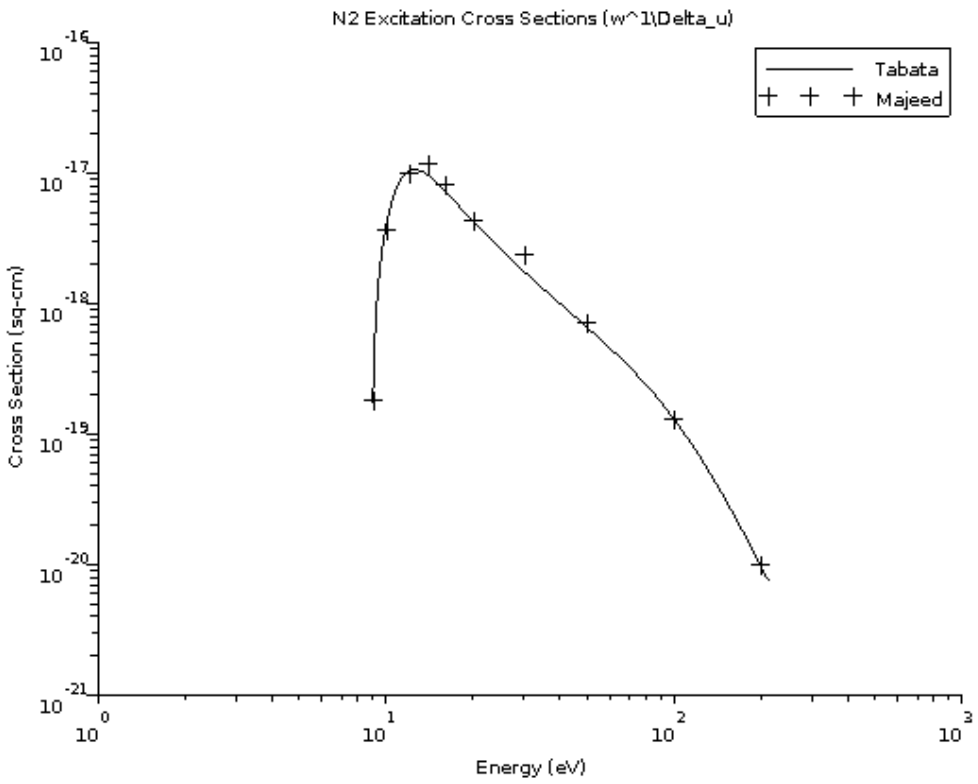


*Figure 5.14*: $w^1\Delta_u$ Excitation Cross Section.

$$\sigma_{w^1\Delta_u} = \frac{\sigma_0 c_1 \left(\frac{(E-E_{th})}{E_R}\right)^{c_2}}{1+\left(\frac{(E-E_{th})}{c_3}^{c_2+c_4}\right)+\left(\frac{(E-E_{th})}{c_5}^{c_2+c_6}\right)} \tag{5.14}$$

*Table 5.14*: Parameters from Tabata [29] for Equation 5.14.

| $E_{th}$ | $c_1$ | $c_2$ | $c_3$ | $c_4$ |
|---|---|---|---|---|
| $8.89E-3$ | $1.22E+0$ | $1.361E+0$ | $3.77E-3$ | $1.43E+0$ |
| | $c_5$ | $c_6$ | | |
| | $2.13E-2$ | $4.51E+0$ | | |

# Chapter 6

# ELECTRON IMPACT IONIZATION OF MOLECULAR NITROGEN

## 6.1 Introduction

In Chapter 5 the analytic forms from Tabata [29] of cross sections for excitation to discrete states of molecular nitrogen by electrons were presented. Chapter 4 analytic forms for elastic scattering cross sections of molecular nitrogen for electrons from both Jackman[16] and Tabata[29] were presented. A complete set of cross sections for the most likely interactions between electrons and nitrogen molecules requires ionization cross sections consistent with the elastic scattering and excitation cross sections presented in previous chapters. Fortunately, Tabata provides an analytic form for total ionization cross section of molecular nitrogen for electrons and Jackman, Garvey, and Green [10] provide analytic forms of the cross sections of individual ionizations states. Utilization of the cross sections from these two works in conjunction with the previously presented cross sections allows development of a Monte Carlo experiment in which not only the type of interaction (elastic, excitation, or ionization) can be determined but the the states of excitation or ionization can be determined as well. Jackman, Garvey, and Green [10] also provide the doubly differential cross sections for electron impact ionization of molecular nitrogen by which the energy spectrum of secondary electron emissions can be sampled. Finally, the work of Jackman and Green [17] provides cross sections for selection of the deflection angles of secondary electrons ejected in ionization events.

## 6.2 Cross Sections for the Ionization States Of The Nitrogen Ion

Jackman, Garvey, and Green [10] provide parameters for the analytic form from the earlier work of Green and Sawada [13] to generate cross sections for electron impact ionization of resulting in specific states of the nitrogen molecule. In this section, the form of Green and Sawada is presented along with the suggested parameters for each state as suggested by Jackman, Garvey, and Green.

### 6.2.1 The Green-Sawada Form

Green and Sawada [13] begin with a functional representation, equation 6.1, for the differential ionization cross section that take both the energy of the primary electron and the energy of the emitted secondary electron as parameters. They then assert for their cases, oxygen and nitrogen, the parameter $\kappa$ equals 1. Furthermore, they provide a form dependent on only the primary electron energy by integrating the secondary energy, T, over the range 0 to $T_m$ where $T_m$ is half the difference of the primary electron energy and the ionization level threshold energy.

$$S(E,T) = A(E)\left(\frac{\Gamma(E)^2}{(T-T_0(E))^2+\Gamma(E)^2}\right)^{\kappa} \tag{6.1}$$

$$\sigma_s(E) = A(E)\Gamma(E)\left(tan^{-1}\left(\frac{T_m-T_0(E)}{\Gamma(E)}\right)+tan^{-1}\left(\frac{T_0(E)}{\Gamma(E)}\right)\right) \tag{6.2}$$

$$A(E) = \frac{K}{E}ln\frac{E}{J}(10^{-16}) \tag{6.3}$$

$$\Gamma(E) = \frac{E\Gamma_s}{E+\Gamma_b} \tag{6.4}$$

$$T_0(E) = T_s - \frac{1000.0}{E+T_b} \tag{6.5}$$

### 6.2.2 The Jackman-Garvey-Green Parameters For $N_2$ Ionization Cross Sections

*Table 6.1*: Parameters from Jackman, Garvey and Green [10] for Equation 6.2.

| *state* | $I$ | $J$ | $K$ | $\Gamma_s$ | $\Gamma_b$ | $T_s$ | $T_b$ |
|---|---|---|---|---|---|---|---|
| $X^2\Sigma_g$ | 15.58 | 1.74 | 2.42 | 13.8 | 15.58 | 4.71 | 31.16 |
| $A^2\Pi_u$ | 16.72 | 1.74 | 1.06 | 13.8 | 16.73 | 4.71 | 33.46 |
| $B^2\Sigma_u$ | 18.75 | 1.74 | 0.551 | 13.8 | 18.75 | 4.71 | 37.50 |
| $C^2\Sigma_u$ | 23.6 | 1.74 | 0.371 | 13.8 | 23.6 | 4.71 | 47.2 |
| $D^2\Pi_g$ | 22.0 | 1.74 | 0.371 | 13.8 | 22.0 | 4.71 | 44.0 |
| $40eV$ | 40.0 | 1.74 | 0.53 | 13.8 | 40.0 | 4.71 | 80.0 |

### 6.2.3 The Tabata Shiraz Sataka Kubo Form

Tabata et al. [29] provide an analytic expression for the total cross section shown in equation 6.6. Since they also provided the forms for total elastic and excitation cross sections, a complete set of cross sections is available for Monte Carlo selection of interaction type. However, determining the state of the ionized molecule requires the Jackman Green forms. Therefore it is important the sum of cross sections for the individual states obtained via the Jackman Green method approximates the total ionization cross section obtained via the Tabata et al. method.

$$\sigma = \frac{\sigma_0 c_1 ln\left(\frac{E}{E_{th}} + c_2\right)}{E_{th}E\left(1 + \frac{c_3}{E - E_{th}}\right)^{c_4}} \tag{6.6}$$

*Table 6.2*: Parameters from Tabata [29] for equation 6.6.

| $E_{th}$ | $c_1$ | $c_2$ | $c_3$ | $c_4$ |
|---|---|---|---|---|
| $1.56E-2$ | $3.46E-3$ | $7.0E-2$ | $5.75E-2$ | $1.023E+0$ |

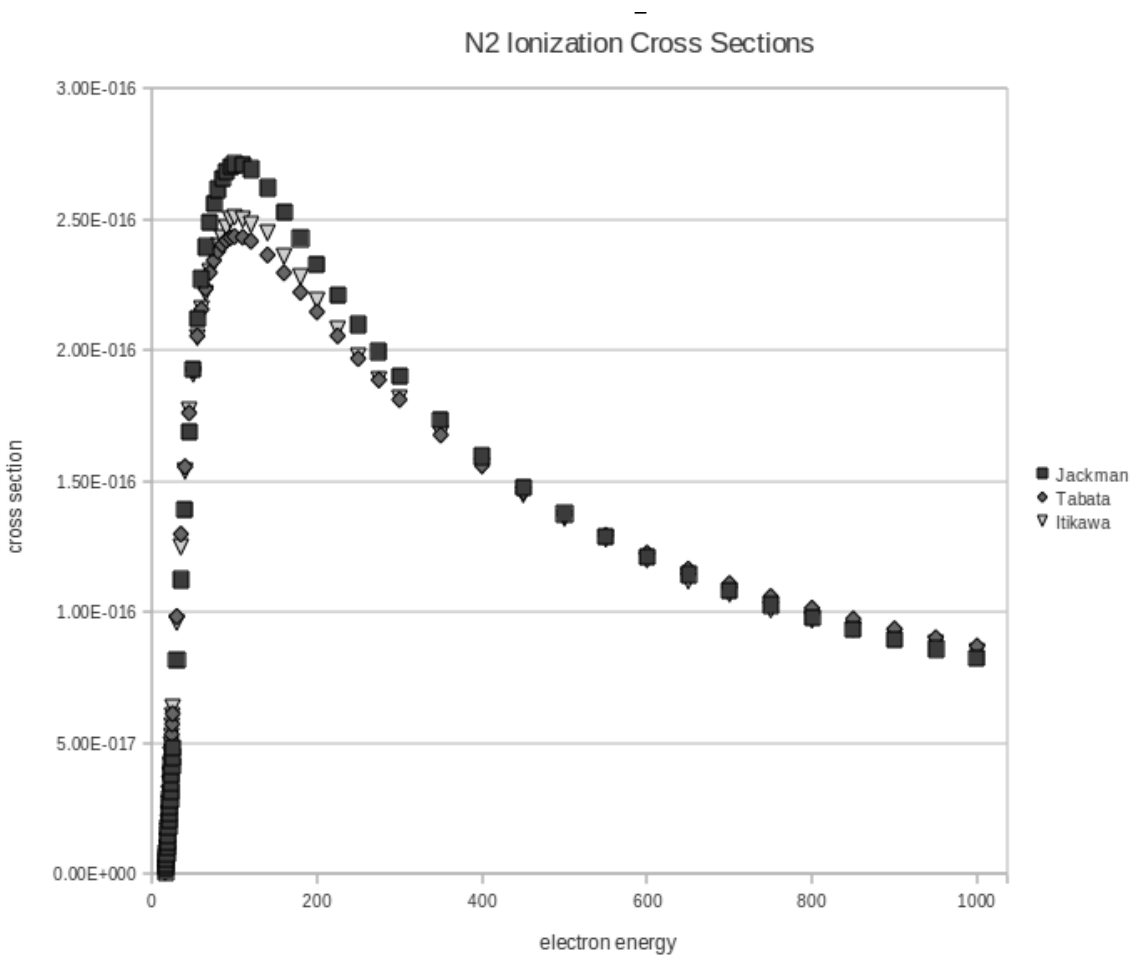


*Figure 6.1*: Total Ionization Cross Sections.
Comparison of the JGG [10] and TSSK [29] analytic forms and the recommended values from Itikawa[15]

### 6.2.4 Comparison Of Forms To Recommended Values

Figure 6.1 shows the sum of the individual ionization states obtained via the Jackman et al. [10] method to be in good agreement with both the total ionization cross section obtained via the Tabata et al. [29] method and the recommended data of Itikawa [15]. However, inspection of the cross sections at higher energies in Figure 6.2 reveals the form fails to converge to twice the atomic cross section. However, it has been discovered through this work a scaling factor can be applied to the Tabata form that maintains the agreement with the recommended data at classical energies while converging with twice the atomic cross section at relativistic energies. The factor is given as $1+3.10x10^{-6}E$ where E is the electron energy.

$$\sigma_{\chi} = \sigma_{Tabata}(1+3.10x10^{-6}E) \tag{6.7}$$

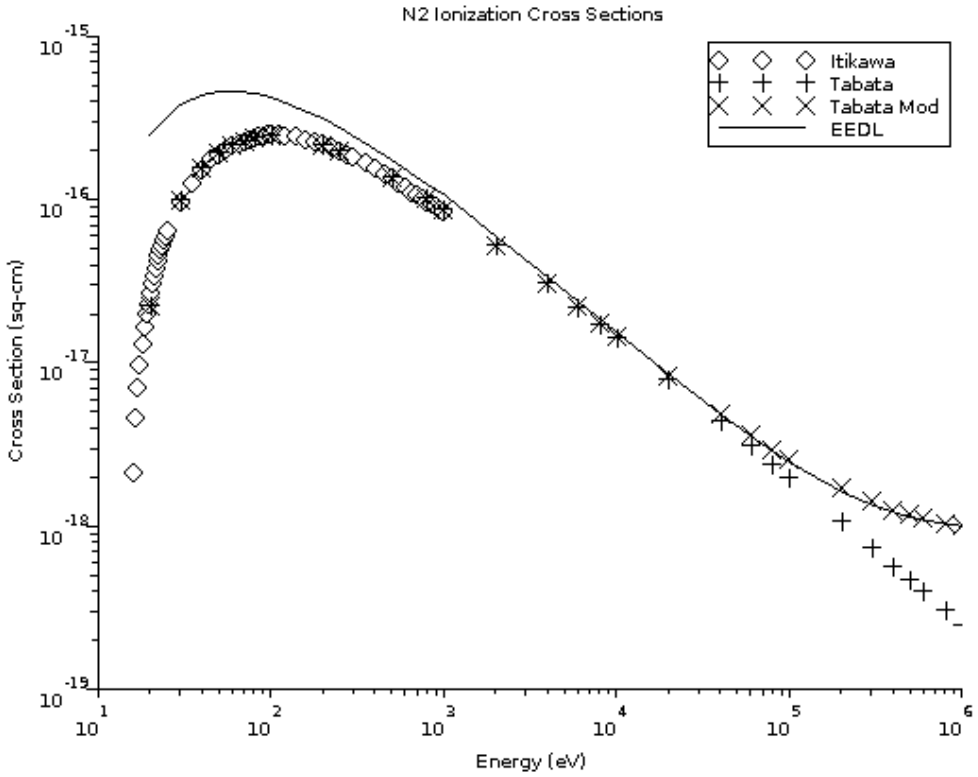


*Figure 6.2*: Total Ionization Cross Sections.
Comparison of the JGG [10] and TSSK [29] analytic forms and the recommended values from Itikawa[15] and 2x EEDL atomic cross sections

## 6.3 The Secondary Electron Energy Spectrum

In section 6.2 the form for the individual excitation states of the molecular nitrogen ion were presented. In this section, account is taken for the the energy loss experienced by the primary electron due to the kinetic energy of freed secondary electron. Since secondary electrons can consume up to half of the primary electron's energy, a secondary electron energy spectrum is needed for the Monte Carlo simulation. One approach is that of Arqueros et al. [1], an extension of the distribution from Opal et al. [22], provides the differential total ionization cross section with respect to secondary electron energy. An alternative approach is taken in this work: the parameters of Jackman et al. [17] as listed in section 6.2.2, are applied to the form of equation 6.1, which can be integrated over $dT$ to produce a cumulative secondary electron distribution as shown in equation (10) of the Green and Sawada paper [13].

## 6.4 Preferential Directions of Secondary Electrons

The work of Jackman and Green [17] utilizes the Green Sawada form of equation 6.1 to provide an analytic fit to the data of Opal et al. [22] for the doubly differential secondary electron cross sections as listed in equations 6.8 - 6.12. Figures 6.3 - 6.5 present cross sections generated for three primary electron energies (100eV, 500eV, 1keV) for four angles each (45,75,105,135) along with reference data from Opal et al. [22].

$$\frac{d\sigma}{dTd\Omega} = \frac{S(E,T)C(T)^2}{[C(T)^2 + B(E)(cos(\theta) - cos(\theta_0(E,T)))^2]N_f(E,T)} \tag{6.8}$$

$$B(E) = 0.0448 + \left(\frac{E}{72900}\right)^{0.91} \tag{6.9}$$

$$C(T) = \frac{36.6}{T + 183} \tag{6.10}$$

$$\theta_0(E,T) = 0.873 + \frac{20 + 0.042E}{T + 28 + 0.066E} \tag{6.11}$$

$$N_f(E,T) = \frac{-2\pi C}{B^{0.5}}\left(tan^{-1}\left(\frac{-B^{0.5}(1+cos(\theta_0)}{C}\right) - tan^{-1}\left(\frac{B^{0.5}(1-cos(\theta_0)}{C}\right)\right) \tag{6.12}$$

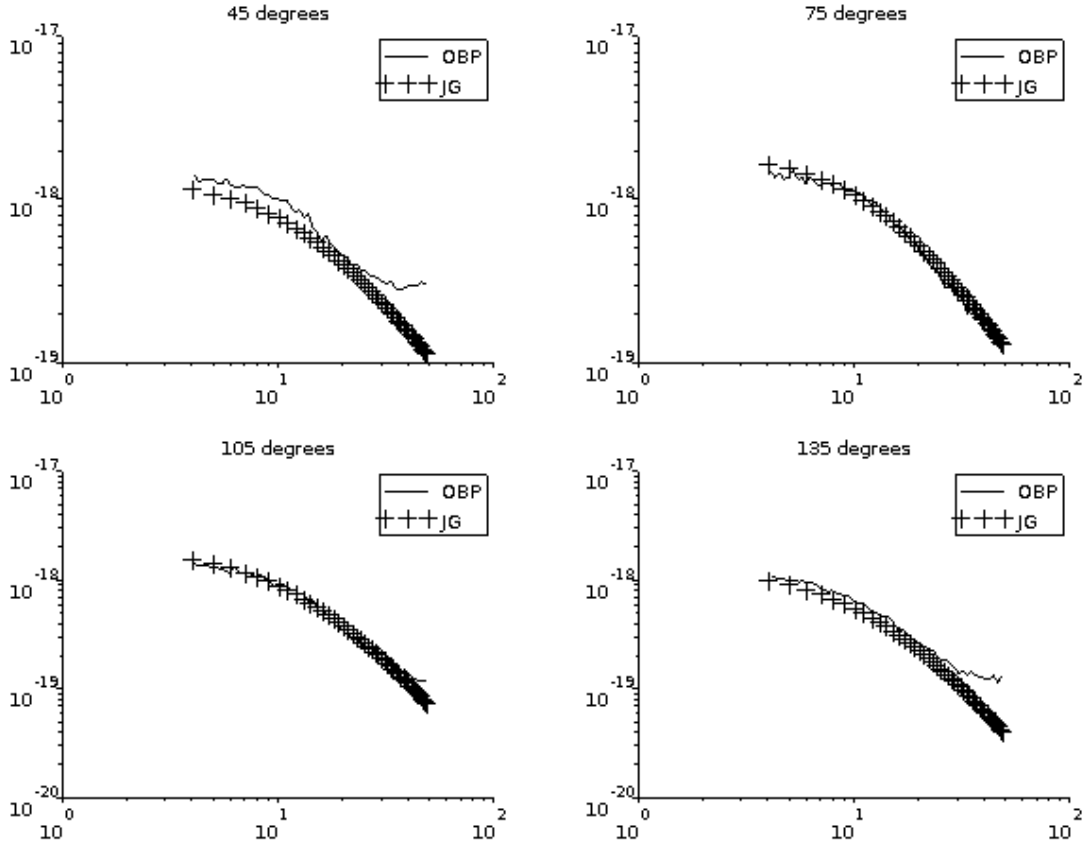


*Figure 6.3*: Differential Ionization Cross Sections, 100eV, (45°,75°,105°,135°).
Cross sections generated for three primary electron energies 100eV for four angles (45°,75°,105°,135°) along with reference data from Opal et al. [22].

## 6.5 Summary

This chapter provides the analytic form for total ionization cross sections of molecular nitrogen for electrons as given by Tabata et al. [29] and the analytic forms for the individual states of the $N_2^+$ ion from Jackman et al. [17]. The cross sections for individual states were summed and plotted along with the total ionization cross sections via Tabata and recommended values from Itikawa [15]. Analytic forms form for both the secondary electron energy spectrum and preferential direction were described and the doubly differential cross sections for secondary electron directions were plotted along with reference data.

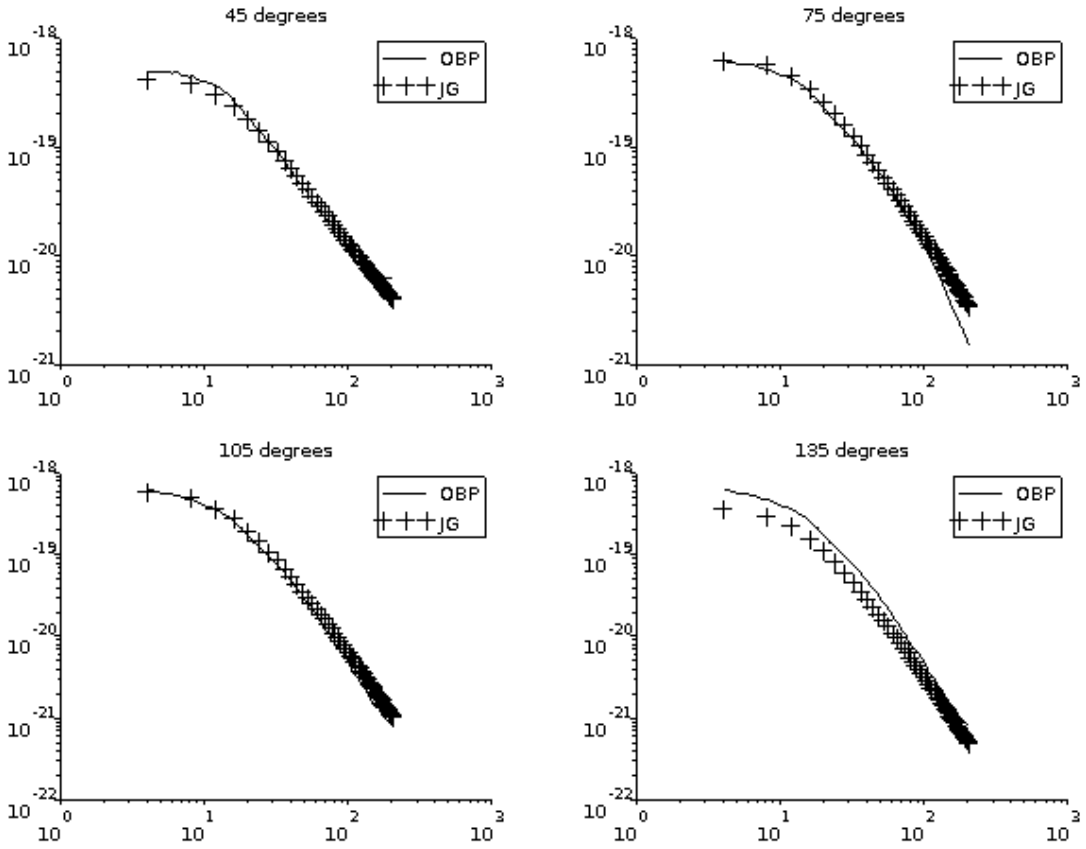


*Figure 6.4*: Differential Ionization Cross Sections, 500eV, (45°,75°,105°,135°).
Cross sections generated for three primary electron energies 500eV for four angles (45°,75°,105°,135°) along with reference data from Opal et al. [22].

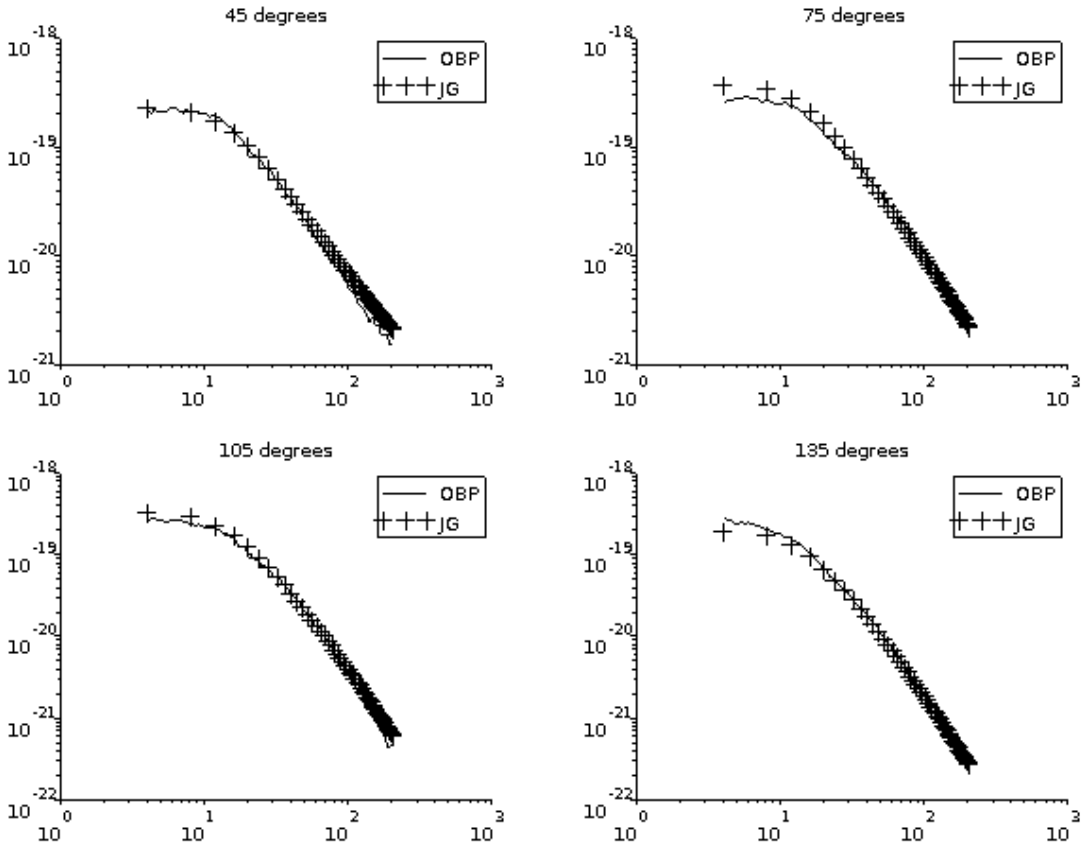


*Figure 6.5*: Differential Ionization Cross Sections, 1000eV, (45°,75°,105°,135°).
Cross sections generated for three primary electron energies 1000eV for four angles (45°,75°,105°,135°) along with reference data from Opal et al. [22].

# Chapter 7

# TOTAL CROSS SECTION OF MOLECULAR NITROGEN FOR ELECTRONS

The previous three chapters have provided analytic forms for the elastic, excitation, and ionization cross sections of nitrogen and their various partial and differential cross sections. In this chapter the sum of the elastic, excitation, and ionization cross sections is compared an analytical expression for the total cross section and recommended values for the total cross section of molecular nitrogen. Additionally, Tabata provides an analytic form for the total $N_2 - e$ cross section, equation 7.1 that is computationally advantageous when computation of the partial cross sections are not required. In this chapter the analytic form for the total cross section is compared to both the sum of the partial cross sections and the recommended values for total cross sections as provided by Itikawa [15].

$$\sigma_T = \frac{\sigma_0 c_1 \left(\frac{(E-E_{th})}{E_R}\right)^{c_2}}{1+\left(\frac{(E-E_{th})}{c_3}^{c_2+c_4}\right)+\left(\frac{(E-E_{th})}{c_5}^{c_2+c_6}\right)} + \frac{\sigma_0 c_7 \left(\frac{(E-E_{th})}{E_R}\right)^{c_8}}{1+\left(\frac{(E-E_{th})}{c_9}^{c_8+c_{10}}\right)} \tag{7.1}$$

*Table 7.1*: Parameters from Tabata [29] for Equation 7.1.

| $E_{th}$ | $c_1$ | $c_2$ | $c_3$ | $c_4$ |
|---|---|---|---|---|
| 0.0 | $6.13E+4$ | $1.53+0$ | $3.11E-5$ | $-1.54E-1$ |
| | $c_5$ | $c_6$ | $c_7$ | $c_8$ |
| | $9.31E-4$ | $8.77E-1$ | $9.17E+7$ | $8.32E+0$ |
| | $c_9$ | $c_{10}$ | | |
| | $2.362E-3$ | $6.05E+0$ | | |

The parameters from Table 7.1 are used in equation 7.1 to calculate the total cross sections for electron interactions with molecular nitrogen. The result is plotted in Figure 7.1 along with the cross sections for elastic scattering, excitation, and ionization as calculated in previous chapters. Additionally, the sum of the elastic scattering, excitation, and ionization cross sections is plotted along with the recommended total cross section values from Itikawa [15] in Table 7.2.

*Table 7.2*: Recommended Total $N_2$-e Cross Sections from Itikawa [15].
(Cross sections are given in units of $10^{-16} cm^2$).

| E | TCS | | E | TCS | | E | TCS |
|---|---|---|---|---|---|---|---|
| 12 | 12.4 | | 60 | 10.7 | | 300 | 5.04 |
| 15 | 13.2 | | 70 | 10.2 | | 350 | 4.54 |
| 17 | 13.5 | | 80 | 9.72 | | 400 | 4.15 |
| 20 | 13.7 | | 90 | 9.3 | | 450 | 3.82 |
| 25 | 13.5 | | 100 | 8.94 | | 500 | 3.55 |
| 30 | 13.0 | | 120 | 8.33 | | 600 | 3.14 |
| 35 | 12.4 | | 150 | 7.48 | | 700 | 2.79 |
| 40 | 12.0 | | 170 | 7.02 | | 800 | 2.55 |
| 45 | 11.6 | | 200 | 6.43 | | 900 | 2.32 |
| 50 | 11.3 | | 250 | 5.66 | | 1000 | 2.16 |

An analytic form for total cross section is of value in calculations that require only the total cross section value. In this chapter, the sum of the cross sections for the dominate electron interactions with molecular nitrogen was compared to an analytic expression from Tabata et al. These cross sections were also shown to be in good agreement with the recommended cross section values from Itikawa.

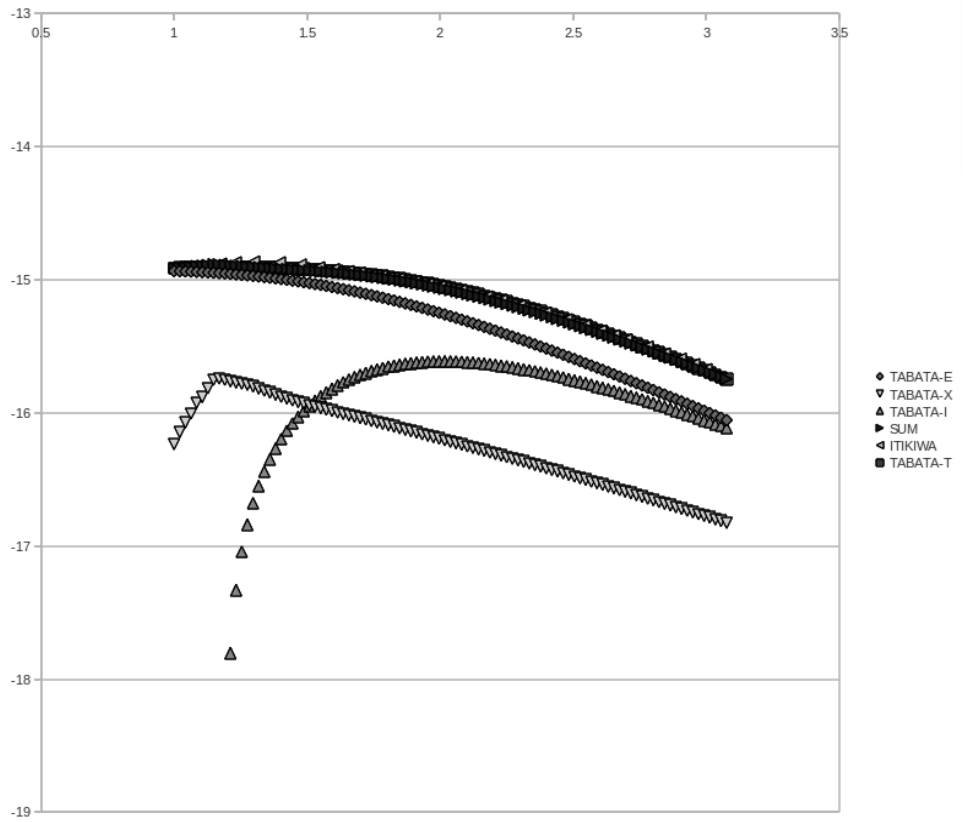


*Figure 7.1*: Comparison of $N_2$-e Cross Sections.
The analytic forms for elastic, excitation, and ionization cross sections are plotted. The sum of those three forms is also plotted along with the analytic form for the total cross section and the recommended values for total cross sections.

# Chapter 8

# DEVELOPMENT OF AN AGENCY

## 8.1 Introduction

A migration from monolithic software applications installed on users computers to distributed Internet based applications is well under way. In the past decade, the Internet has evolved from a graph of linked static content to a communication channel for dynamic systems that expose web-services and provide access to cloud based applications. Service Oriented Architecture (SOA) and Software as a Service (SaaS) are software design and deployment paradigms for Internet based software. These techniques rose to prominence in the early 2000s and were quickly adopted for enterprise and consumer applications. SOA and SaaS are slowly gaining a foothold in the scientific community. The primary goal of this work is application of software engineering and development techniques from the enterprise sector to a scientific domain; providing a new paradigm for scientific software development through a fusion of modular software methodology and distributed computing techniques. An agent-based paradigm utilizing a distributed modular framework for Monte Carlo simulation provides higher levels of flexibility that traditional design techniques. The paradigm developed in this work marks a departure from the methodologies of traditional Monte Carlo simulation where the cost of computational resources and the complexities of modeling physical systems often required simplifications of both the models and the simulations. Modern hardware and development techniques provide capabilities for modular design methodologies, encourages development of reusable software components, and utilize sophisticated build management tools.In this chapter, the design of the agency constructed as part of the electron impact induced air fluorescence case study is reviewed.

## 8.2 A Component Model Framework

### 8.2.1 OSGi

In the late 1990s, many people envisioned a future filled with Internet capable gadgetry. In the following decade, consumer demand for Internet-related technologies produced a plethora of Internet-enabled consumer devices, many of which use Sun Microsystem's Java platform. In 1999, the Open Source Gateway initiative was formed as an alliance between

Sun Microsystems and device manufactures such as Ericsson and Motorola and provides an open standard for modular Java development. Currently, over a hundred organizations are either members or supporters of the OSGi Alliance.

Eclipse is a software development environment originally developed by IBM and made open source in 2001. Since 2004, Eclipse has been developed and maintained by a non-profit consortium that currently consists of nearly two hundred companies. In 2004, the Eclipse Foundation decided version 3.0 of Eclipse would abandon its custom plug-in architecture and develop a new modular architecture adhering to the OSGi standard [14]. The Eclipse Foundation's implementation of the OSGi specification is named Equinox and is currently the certified reference implementation of the specification. It is available from the Eclipse Foundation website and is licensed under the Eclipse Public License.

The OSGi framework is one of the core components of the agency. OSGi facilitates development of loosely coupled modular components, allowing building of complex systems from a collection of simpler components. In the case study, bundles are used to encapsulate specific sets of physical concepts.

## 8.3 A Multi-Agent Framework

### 8.3.1 JADE

There are a number of way to go about designing and implementing agents. Rather than reinventing much of what has been already done, an effort is made to leverage existing tools. In this work, a third part multi-agent framework is utilized for the specifics of agent implementation. JADE is an agent framework for the Java programming language that is developed and maintained by Telecom Italia (TILAB). It is described as "the middleware developed by TILAB for the development of distributed multi-agent applications based on the peer-to-peer communication architecture" [5]. In the context of this work, JADE is the framework that provides common agent capabilities.

### 8.3.2 JADE-OSGi

TILAB provides an OSGi bundle for embedding the JADE framework into an OSGi container. Use of the JADE-OSGi bundle allows development of software with the loosely coupled modularity of OSGi and the distributed architecture of JADE.

## 8.4 Component Deployment and Distribution

As previously mentioned, component deployment and distribution capabilities are required in addition to the basic hosting of agents. Deployment is made possible through integration of an embedded file transfer server. Developers may transfer components to and from the agency via FTP. Additionally, OSGi has a mechanism by which remote bundles can be accessed and installed over HTTP. Sharing components among agencies is accomplished via this mechanism in conjunction with an embedded HTTP server.

## 8.5 Summary

In this work the agency has two requirements in addition to the requirement of hosting agents: provide developers the ability to publish components to the agency and provide a mechanism to retrieve components from the agency for both developers and other agencies. This work provides an agency deployed as a stand-alone Java executable and a set of third party JARs (Java ARchive files). The agents of this work are developed as OSGi bundles and the agency is an extension of an OSGi framework. Specifically, the agency here uses the Equinox framework contained in the Eclipse Foundation's OSGi implementation bundle. During the agency launch, additional bundles are loaded to provide additional agency capabilities. The JADE framework is accessed via the JADE-OSGi bundle through the OSGi framework. The agency executes inside a Java virtual machine and inside the agency are three core components: an OSGi framework, a FTP server, and a HTTP server. All three components are fully embedded in the agency application. The JADE bundle is dynamically loaded into the the OSGi framework at a run-time and handles the traditional core agency functionalities such as agent communication and mobility. The FTP server, and the HTTP server share a common root directory. This configuration allows the agency to act as a repository to which agents and agent components can be deployed and from which they may be distributed to other agencies.Researchers can develop agents and components using an integrated development environment and deployment management tools to deploy agents and components over FTP directly to the agency's repository. Remote agencies can access the repository via the built-in HTTP server.

# Chapter 9

# BASIC MODULES FOR PROOF OF CONCEPT

## 9.1 Electron Beans

The primary actor in the case study is the electron. Almost all other higher level bundles of the case study require a representation of the electron. Therefore, the electron is implemented as a decoupled component that can be used by other components. This chapter provides descriptions of the data structure representation of the electron, its packaging, and deployment. A minimalist object oriented representation is selected for the electron: three member variables representing the three components of its position, another three member variables representing the direction of its momentum vector, an a single member variable representing its kinetic energy. While a real electron also has attributes such as charge, spin, and mass, they are not required in the computations of th case study and are therefore omitted.

## 9.2 The Green Sawada Forms

A motivation in the the case study is careful separation of the various concepts and theories in a complex simulation. Chapter 6 notes that the analytic forms of Green and Sawada [13] are used by Jackman and Green [17] to fit the data of Opal et al. [22]. Jackman and Green indeed provide parameters to Green and Sawada's form to fit the Opal data for electron impact ionization of molecular nitrogen. The form of Jackman and Green is not specific to nitrogen or to the work of Green and Sawada. To avoid either inclusion of all derivative works into a component representing the form of Green and Sawada or replication of the Green and Sawada form in all modules of derivative works, the Green and Sawada forms are encapsulated in their own decoupled module that can be accessed by modules representing derivative works. The module implements equations 4, 5, and 10 from [13] to provide the $\sigma$(E), $\sigma$(E,T), and $\int_{T_i}^{T_f} \sigma$(E,T)dT. As in the case of the electron module, the Java object is package as a JAR file including OSGi headers in its manifest.

## 9.3 The Tabata Shirau Sataka Kubo Forms

Tabata et al. [29] define a set of equations that they then combine in various combinations with different parameters to generate a variety of analytic cross sections. While these equations are specific to the work of Tabata et al., it is desirable to break each type of cross section out into its own bundle. These leads to a similar situations as before. Therefore, the core equations are extracted and placed in their own bundle. Bundles that implement a specific form of the cross sections will depend on this decoupled bundle.

## 9.4 The Quaternion

There are several methods for computing three dimensional rotations including the Euler Method and quaternions. Since the interaction of an electron and a molecule causes a deflection of the electron trajectory, a rotation method is required for computing the direction of the electron trajectory after the interaction. For the purposes of the current work, the quaternion method is selected. The quaternion method is not specific to any process in the simulation and therefore merits its own bundle.

## 9.5 Packaging

The Java objects are packaged in JAR files and the only difference from ordinary Java Beans packaged in JAR files is the content of the JAR manifests. OSGi headers in the manifest are used to declare the bundle name, version, and the packages that OSGi should make available to other bundles.

## 9.6 Deployment

There are a number of ways the bundles could be deployed. In the course of the case study three primary methods were utilized: manual copy, FTP, and the build management tool Maven. In the cases of FTP and Maven, the upload directory points to the directory monitored by the Apache FileInstall bundle and installation of the uploaded bundle is automatic.

## 9.7 Summary

This chapter provided three examples in which low level bundles are utilized in the case study. In all three example, the component implements some functionality that would

otherwise be either replicated or absorb excessive external influence. The presented method achieves a balance of granularity and re usability.

# Chapter 10

# AGENTS FOR NITROGEN-ELECTRON INTERACTIONS

## 10.1 Introduction

In this chapter, descriptions are given for the agents that compute the various cross sections and perform basic simulation tasks. These are the agents that provide the basic behaviors required in a simulation of electron interactions with nitrogen molecules. In Chapter 11, a higher level agent will be introduced that utilizes the capabilities of the agents described in this chapter. Chapter 12 will present a high level agents that coordinate these agents and the agent to be introduced in Chapter 11 to conduct simulations of various scenerios in which electrons interact with nitrogen molecules.

## 10.2 Elastic Scattering

There are two basic agents for elastic scattering interactions. The first agent is responsible for computing the molecular nitrogen cross section for an electron of a given energy. The second elasric scattering agent conducts Monte Carlo experiments to select the angle by which the incident electron is deflected.

### 10.2.1 Total Elastic Cross Section

The agent responsible for computation of the total elastic electron impact cross sections for molecular nitrogen publishes a JADE service description advertising its capability to calculate those cross sections. Other agents may discover this agent by querying the JADE directory for the published service description. Upon receipt of a FIPA ACL message, the content of the message is parsed for the enclosed electron energy. The agent is dynamically linked via OSGi to the bundled implementation of the Tabata forms described in Chapter 9. The agent uses the Tabata form for the total elastic electron impact cross section of molecular nitrogen to compute the cross section at the electron energy specified in the received message. The agent then creates a reply message, encloses the computed cross section, and sends the message to the requesting agent.

### 10.2.2 Differential Elastic Cross Section

The agent responsible for computation of differential elastic electron impact cross sections for molecular nitrogen actually performs the simulation of the scattering event. Rather than publishing a JADE service description advertising a service for calculating a cross section, it registers a service description indicating it simulates elastic scattering events for electron collisions with nitrogen molecules. This agent expects serialized electron data structures as the content of incoming messages. The agent implements the analytic form for differential elastic electron impact cross sections of Jackman and Green [17] and utilizes that form in a Monte Carlo selection of scattering angle. The OSGi quaternion module introduced in Chapter 9 is used by the agent to apply the deflection to the electron. The electron is then serialized and package in a reply that is sent to the requesting agent.

## 10.3 Excitation

The agent responsible for computation of the excitation electron impact cross sections for molecular nitrogen publishes three JADE service descriptions advertising the ability to compute the total excitation electron impact cross section for molecular nitrogen, the ability to perform a Monte Carlo selection of the excited state, and the ability to provide the quantity of energy lost by the impact electron in a specific excitation event. Since the agent provides three services, it expects specification of requested service within incoming messages.

### 10.3.1 Monte Carlo Selection Of Excited State

If the incoming request specifies selection of excited state, the agent extracts the electron energy from the received message and computes the the excitation cross section for each state of the nitrogen molecule via the OSGi module implementation of the Tabata forms. The cross sections are then used to construct a cumulative probability distribution that is sampled by a Monte Carlo algorithm. The identifier for the sampled excitation state is then encoded into the reply message and sent to the requesting agent.

### 10.3.2 Energy Loss

An agent can request the amount of energy lost in an excitation event. When the excitation agent receives the request, it looks up the energy threshold for the specified event, encodes the result in a reply message, and sends the reply to the requesting agent.

### 10.3.3 Total Excitation Cross Section

When the agent receives a request for a total excitation cross section, it first extracts the electron energy from the incoming request and computes the the excitation cross section for each state of the nitrogen molecule via the OSGi module implementation of the Tabata forms. The agent then sums the computed cross section and returns the result in a message to the requesting agent.

## 10.4 Ionization

The processes related to electron impact ionization of molecular nitrogen are distributed over three agents. The first agent handles requests for total ionization cross section. The second agent handles three types of requests: Monte Carlo selection of ionization state, Monte Carlo selection of secondary electron energy, and energy quantity lost by an incident electron for a particular ionization interaction. The third agent handles requests for the preferred direction of a secondary electron ejected in an ionization event.

### 10.4.1 Total Ionization Cross Section

Upon receipt of a request for a total ionization cross section, the agent accesses the algorithm from Tabata that is included in an OSGi bundle as previously described. The energy from the the incoming message is passed to the algorithm and total ionization cross section is computed, encoded in the reply message, and sent to the requesting agent.

### 10.4.2 Monte Carlo Selection Of Ionization State

The agent responsible for Monte Carlo selection of ionization state implements the analytic ionization state cross section forms of Jackman, Garvey, and Green [10] which depend on the OSGi bundle that implements the forms of Green and Sawada [13]. The cross sections are computed for each of the ionization states and those cross sections are used to form a cumulative probability distribution. The Monte Carlo method is used to sample the probability and the identifier corresponding to the sampled state is returned. The agent encodes the state identifier in a reply message that is sent to the requesting agent.

### 10.4.3 Monte Carlo Selection Of The Secondary Energy

The energy distribution of secondary electrons is dependent on the residual state of the ion. The agent responsible for Monte Carlo selection of energy for a secondary electron first computes the energy range for the specified state of the molecular nitrogen ion. Then

a recursive binary partitioning method is employed in which the Jackman-Garvey-Green parameters are passed to the Green-Sawada form for integrated secondary energy. The energy ranges are specified for each of the two bins and one bin is selected via the Monte Carlo method. While the width of the selected energy bin is greater than the chosen minimum secondary electron energy, the bin is recursively divided and subjected to Monte Carlo selection. The center energy of the resulting bin is selected as the secondary electron energy, encoded into a reply, and sent to the requesting agent.

### 10.4.4 Energy Loss To Ionization

When the agent receives a request for energy loss due to an ionization event, the agent looks up the threshold value associated with the specified ion state. The value is enclosed in a reply message and sent to the requesting agent.

### 10.4.5 Secondary Electron Direction

The range of possible angles is partitioned into bins and the cross section for each angular range is computed according to the method of Jackman and Green [17]. The computed cross sections are used to construct a cumulative probability distribution that is sampled according to the Monte Carlo method. The center angle of the selected bin is returned as the preferred scattering angle of the ejected electron. The angle is enclosed in a reply to the request and is sent to requesting agent.

## 10.5 Scattering of Primary Electrons Via Ionization and Excitation

In both ionization and excitation events, the primary electron energy is reduced by the amount of energy lost in the interaction. The electron with reduced energy is then subjected to elastic scattering.

## 10.6 Summary

This chapter provides an overview of agents designed to handle the various interaction of electrons and nitrogen molecules. Agents for the three dominant interactions at energies less 1 MeV are presented. In all cases, deflection angles for primary electrons are treated as elastic scattering event. This approximation is sufficient for the current work but may not be suitable in other cases. Room is left for future improvements in this area.

# Chapter 11

# AN AGENT FOR MONTE CARLO SELECTION OF NITROGEN-ELECTRON INTERACTIONS

This chapter describes the development of an agent that utilizes the agents previously discussed to perform Monte Carlo selection the type of interaction that occurs between an electron and a nitrogen molecule. This agent is also responsible for coordinating those agents to determine the consequences of the selected interaction. The selection agent receives a request containing an electron energy and in turn requests cross sections for the various electron-nitrogen interactions from the other agents. Once the selection agent has received the relevant cross sections, the cross sections are used in a Monte Carlo selection of interaction type. The selection agent then queries the agents related to the selected process to gather information required to determine the consequence of the interaction. A communication diagram for interaction selection and resolution sequence is shown in Figure 11.1. In the first phase, the selection agent requests the total elastic cross section, the total ionization cross section, and the total elastic cross section. The three cross sections are then used in a Monte Carlo selection process. It is important to note that the peer to peer communication among agents is asynchronous and is not required to occur in the order depicted. However, the selection agent must wait for replies to these queries before the Monte Carlo selection can be performed. Once the interaction selection phase is complete, the agent then resolves the effects of the selected interaction. The possible communication paths are illustrated in the communication diagram as shaded conditional block. An elastic scattering interaction is the simplest of the three illustrated processes. In the case of elastic scattering the agent requests the elastic scattering angle. The agent responsible for providing the the scattering angle performs its own Monte Carlo simulation to select the scattering angle according to its elastic scattering model. The computed scattering angle is sent to the selection and resolution agent. In the case of excitation, the selection and resolution agent requests selection of an excitation state. The agent responsible for selecting the excitation state performs a Monte Carlo simulation using its excitation models and send the selected state to the selection and resolution agent. Knowing the selected state, the selection and resolution agent then requests the amount of energy lost to the excitation. After receiving the energy loss value, the electron energy is reduced by that amount and the reduced energy

is sent in a request for elastic scattering angle. Ionization is the most complex of the three interactions. The selection and resolution agent must request the ionization state. The agent responsible for selecting the ionization state conducts its own Monte Carlo simulation to determine the state and the state is sent to selection and resolution agent. As with excitation, the selection and resolution agent requests the amount of energy lost in the inter action and reduces the electron energy by the amount received. The ionization event also produces a secondary free electron. The interaction and selection agent must determine the energy lost to the secondary electron and the secondary electron's direction. Agents carry out Monte Carlo simulations to sample the secondary electron energy spectrum and the angular distribution of ejected electrons. As in the previous cases, the reduced electron energy is used in a Monte Carlo selection of scattering angle. In all cases, the selection and resolution agent provided the details of the selected interaction and the consequences of the interaction to the agent that originally provided the electron for the interaction.

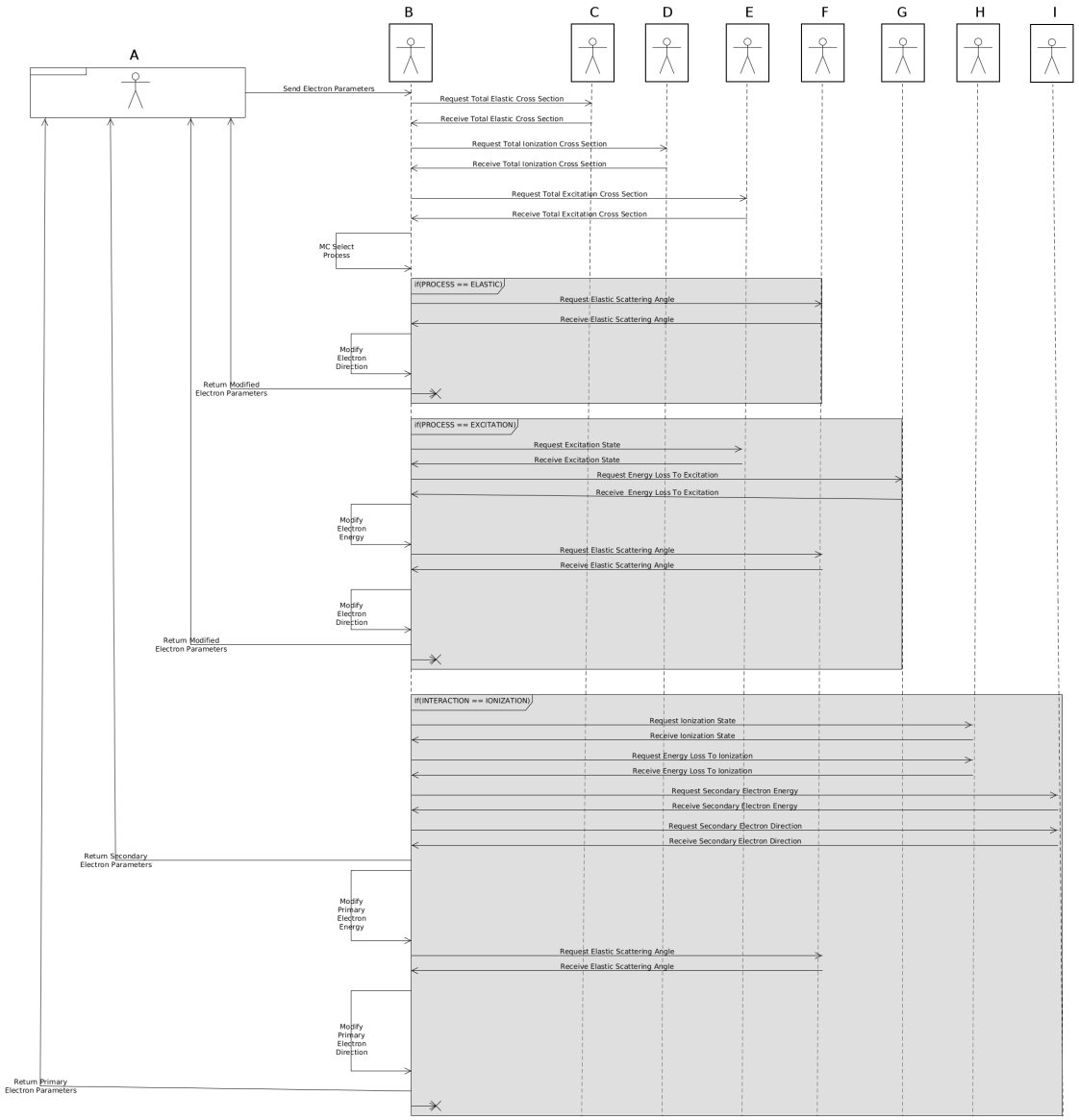


*Figure 11.1*: Selection Agent Communication Diagram.
The communication diagram illustrates the communicative acts between an interaction selection and resolution agent and the community of agents providing the core capabilities.

# Chapter 12

# SIMULATING NITROGEN-ELECTRON INTERACTIONS

## 12.1 Introduction

At this point, agents and bundles encapsulation the theory required for simulation of an low energy electron passing through a volume of molecular nitrogen gas has been presented. Now, additional agents can be constructed to coordinate simulations executed by the agent community. In this chapter, two agents are presented for the purposes of orchestrating simulations of low energy electron interaction with molecular nitrogen. The first agent simulates the interaction of a 1MeV electron with nitrogen and reports the number of occurrences of each type of interaction for the primary electron and all electrons produced in the decay cascade. The second agent tracks only the primary electron keeping a running total of the distances between interaction and reports the total path length of the electron's trajectory.

## 12.2 Simulation I

A simulation was carried out for primary electrons each with a starting kinetic energy of 1MeV. The simulation management agent tallied the occurrences of the various interaction types and the results are shown in Table 12.1. A metric for measuring the performance of the simulation is the average energy expended per ionization event. Summing the occurrences in Table 12.1 over the ionization interactions and normalizing by the total deposited energy yields a value of 34.77 eV per ionization event. In 2010, Wedlund et al. [28] arrived the value 34.3$\pm$1.8 eV per ionization in molecular nitrogen and reference prior experimental values of 34.8$\pm$0.2. Additionally, the work of Waldenmaier et al. [32] suggests electron interactions with molecular nitrogen should result in approximately 1.52 excitations to the $C^3\Pi_u$ state per keV of primary electron energy. The simulation produced 1.81 excitations to the $C^3\Pi_u$ per keV of primary electron energy and is therefore seen in good agreement with the measurements and calculations of Waldenmaier et al. Having good agreement with third party data for both the average energy expended per ion pair and the number of excitations to a particular state provides confidence in the computational system capabilities in modeling electron energy degradation in nitrogen.

*Table 12.1*: The Mean Number of Occurrences of Each Type of Interaction in a Simulation of 1MeV Incident Electrons

| Interaction | Occurrences |
|---|---|
| $a^1\Pi_g$ | 2815.06 |
| $a^1\Sigma_g$ | 345.98 |
| $a^1\Sigma_u$ | 595.58 |
| $A^3\Sigma_u$ | 1653.70 |
| $b^1\Pi_u$ | 3506.9 |
| $b^1\Sigma_u$ | 3532.78 |
| $B^3\Pi_g$ | 1816.24 |
| $B^3\Sigma_u$ | 697.14 |
| $c^1\Pi_u$ | 4743.06 |
| $c^1\Sigma_u$ | 2180.36 |
| $C^3\Pi_u$ | 1806.00 |
| $E^3\Sigma_g$ | 83.24 |
| $w^1\Delta_u$ | 586.68 |
| $W^3\Delta_u$ | 2189.10 |
| $X^2\Sigma_g$ | 13635.36 |
| $A^2\Pi_u$ | 5904.08 |
| $B^2\Sigma_u$ | 2997.14 |
| $C^2\Sigma_u$ | 1901.76 |
| $D^2\Pi_g$ | 1944.90 |
| $40eV state$ | 2369.86 |
| $elastic$ | 14539.28 |

## 12.3 Simulation II

A second simulation was conducted in which the path lengths of primary electrons for each of nine starting energies were reported. Table 12.2 provides the mean path length traversed for electrons of each starting energy. The results are in good agreement with calculations based on the continuous slowing down approximation. At 80keV, the electron velocity is slightly more than half the speed of light. As the energy is increased, relativistic effects become more prominent. Application of a Lorentz contraction to the simulated track lengths produces track lengths in seemingly better agreement with CSDA lengths at all energies (Figure 12.1).

*Table 12.2*: Simulated Electron Track Lengths for Nine Primary Energies.

| Starting Energy | Mean Track Length |
|---|---|
| 10*keV* | 0.26*cm* |
| 20*keV* | 0.84*cm* |
| 40*keV* | 2.76*cm* |
| 60*keV* | 5.92*cm* |
| 80*keV* | 9.33*cm* |
| 100*keV* | 14.59*cm* |
| 250*keV* | 80.75*cm* |
| 500*keV* | 297.94*cm* |
| 1.0*MeV* | 1103.23*cm* |

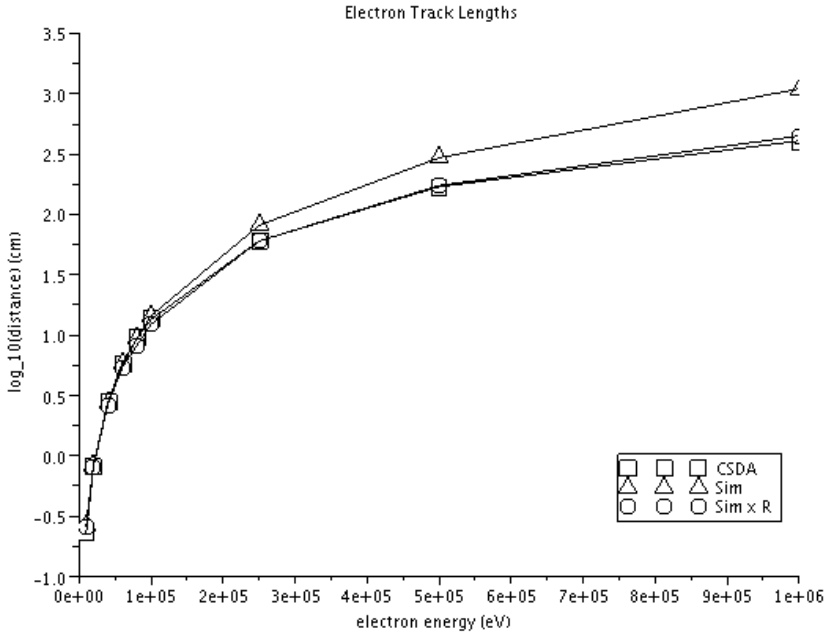


*Figure 12.1*: Comparison of Electron Track Lengths
Application of the Lorentz contraction to the simulated path length brings it into good agreement with the Continious Slowing Down Approximation (CSDA).

# Chapter 13
# CONCLUSION

A paradigm for utilization of mobile agents in a modular architecture has been demonstrated. Software engineering and development techniques from the enterprise sector have been combined in a scientific domain providing a new paradigm for scientific software development through a fusion of modular software methodology and distributed computing techniques. The new paradigm moves agent-based computing beyond the confines of software engineering and into the realm of computing for physical science through presenting the agents as representations of virtual scientists and their behaviors as abilities to perform computational tasks related to a specific scientific objective. The agency should now be viewed as a tool that assists scientists in development, deployment, and management of a community of agents and modular artifacts representing scientific capabilities. Furthermore, an overall system of agencies is envisioned as a community of virtual scientists cooperating to achieve a simulated scientific objective.

Chapters 8 through 12 detailed the development of a system of agents designed to carry out simulations based on the physics detailed in Chapters 3 through 7. Through this process, a analytic forms and reference data from multiple sources have been brought together in a single application. The developed paradigm facilitated the management and integration of these diverse concept. In addition to demonstration of the paradigm's proof of concept, the case study results are of significance. The results of the simulations have been shown in good agreement with accepted values from the literature and have provided valuable insight to the utility of the individual components. While the case study is specific, the techniques employed in addressing the encountered problems are general and applicable to a much broader range of scientific simulation. The result of this work is a paradigm in which the burden of Monte Carlo simulation is lessened through realization of a modular system of agents that may be augmented as a virtual collaborative community.

The future of this work continues on multiple fronts: further refinement and testing of the paradigm, expansion of the case study, development of new studies, and transition to application beyond the lab. The primary objective of a paradigm is to produce a conceptual approach to problem solving in a particular application domain by providing a framework in which it practitioner can develop and manage abstract ideas in a meaningful way. How those practitioners employ the paradigm is a story only time can tell.

# BIBLIOGRAPHY


[1] F. Arqueros. Analysis of the fluorescence emission from atmospheric nitrogen by electron excitation and its application to fluorescence telescopes. *New Journal of Physics*, 11:29, June 2009.

[2] F. Arqueros, F. Blanco, A. Castellanos, M. Ortiz, and J. Rosado. The yield of air fluorescence induced by electrons. *Astroparticle Physics*, 26(4-5):231–242, 2006.

[3] F. Arqueros, F. Blanco, and J. Rosado. Improved model for the analysis of air fluorescence induced by electrons. *Nuclear Instruments and Methods in Physics Research Section A: Accelerators, Spectrometers, Detectors and Associated Equipment*, 597(1):94–98, 2008. Proceedings of the 5th Fluorescence Workshop.

[4] Fernando Arqueros, Jörg R. Hörandel, and Bianca Keilhauer. Air fluorescence relevant for cosmic-ray detection–summary of the 5th fluorescence workshop, el escorial 2007. *Nuclear Instruments and Methods in Physics Research Section A: Accelerators, Spectrometers, Detectors and Associated Equipment*, 597(1):1–22, 2008. Proceedings of the 5th Fluorescence Workshop.

[5] F. Bellifemine, G. Caire, A. Pogg, and G. Rimassa. Jade - a white paper. Technical Report 3, Telecom Italia Lab, EXP Online, 2003.

[6] Fabio Luigi Bellifemine, Giovanni Caire, and Dominic Greenwood. *Developing Multi-Agent Systems with JADE*. Wiley, 2007.

[7] T. Bergmann, R. Engel, D. Heck, N.N. Kalmykov, S. Ostapchenko, T. Pierog, T. Thouw, and K. Werner. One-dimensional hybrid approach to extensive air shower simulation. *Astroparticle Physics*, 26(6):420–432, 2007.

[8] Peter Braun and Wilhelm Rossak. *Mobile Agents*. Morgan Kaufmann, 2005.

[9] Alan Newton Bunner. *The atmosphere as a cosmic ray scintillator.* PhD thesis, Cornell University, 1964.

[10] R. Garvey C. Jackman and A. Green. Electron impact on atmospheric gases, i. updated cross sections. *J. Geophys. Res.*, 82, 1977.

[11] G. Davidson and R. O'Neil. Optical radiation from nitrogen and air at high pressure excited by energetic electrons. *The Journal of Chemical Physics*, 41(12):3946–3955, 1964.

[12] G. Davidson and R. O'Neil. The fluorescence of air and nitrogen excited by energetic electrons. Technical report, American Science and Engineering, Inc., Cambridge, Mass., 1968.

[13] A. E. S. Green and T. Sawada. Ionization cross sections and secondary electron distributions. *Journal of Atmospheric and Terrestrial Physics*, 34(10):1719–1728, 1972.

[14] O. Gruber et al. The Eclipse 3.0 platform: Adopting OSGI technology. *IBM Systems Journal*, 44(2), 2005.

[15] Yukikazu Itikawa. Cross sections for electron collisions with nitrogen molecules. *Journal of Physical and Chemical Reference Data*, 35(1):31–53, 2006.

[16] C. Jackman. *Spatial and energetic aspects of electron energy deposition*. PhD thesis, The University of Florida, 1978.

[17] C. Jackman and A. Green. Electron impact on atmospheric gasses. iii - spatial yield spectra for n2. *J. Geophys. Res.*, 84:2715–2724, June 1979.

[18] J.C. Lee. Radiation-induced phenomena in air: Ionization and fluorescence. *Nuclear Instruments and Methods in Physics Research Section A: Accelerators, Spectrometers, Detectors and Associated Equipment*, 580(1):254–257, 2007. Proceedings of the 10 th International Symposium on Radiation Physics - ISRP 10.

[19] Tariq Majeed and Douglas J. Strickland. New survey of electron impact cross sections for photoelectron and auroral electron energy loss calculations. *Journal of Physical and Chemical Reference Data*, 26(2):335–349, 1997.

[20] Jeff McAffer, Paul VanderLei, and Simon Archer. *OSGi and Equinox: Creating Highly Modular Java Systems*. Addison-Wesley, Upper Saddle River, NJ, 2010.

[21] M. Nagano, K. Kobayakawa, N. Sakaki, and K. Ando. Photon yields from nitrogen gas and dry air excited by electrons. *Astroparticle Physics*, 20(3):293–309, 2003.

[22] C.B. Opal, E.C. Beaty, and W.K. Peterson. Tables of secondary-electron-production cross sections. *Atomic Data and Nuclear Data Tables*, 4:209–253, 1972.

[23] S. Perkins et al. Tables and graphs of electron-interaction cross sections from 10 ev to 100 gev derived from the llnl evaluated electron data library (eedl), z = 1–100. Technical report, U.S. Dept. of Energy, 1991.

[24] Jan S. Rellermeyer, Gustavo Alonso, and Timothy Roscoe. R-osgi: distributed applications through software modularization. In *Proceedings of the 8th ACM/IFIP/USENIX international conference on Middleware*, MIDDLEWARE2007, pages 1–20, Berlin, Heidelberg, 2007. Springer-Verlag.

[25] F. Salvat et al. Penelope – a code system for monte carlo simulation of electron and photon transport. *Nuclear Energy Agency OECD/NEA*, 2001.

[26] Yoav Shoham. Agent-oriented programming. *Artificial Intelligence*, 60(1):51–92, 1993.

[27] T. Shyn et al. Angular distribution of electrons elastically scattered from gases - 1.5-400 ev on n2. *PHYSICAL REVIEW A*, 22(3), 1980.

[28] C. Simon Wedlund, G. Gronoff, J. Lilensten, H. Ménager, and M. Barthélemy. Comprehensive calculation of the energy per ion pair or w values for five major planetary upper atmospheres. *Annales Geophysicae*, 29(1):187–195, 2011.

[29] Tatsuo Tabata, Toshizo Shirai, Masao Sataka, and Hirotaka Kubo. Analytic cross sections for electron impact collisions with nitrogen molecules. *Atomic Data and Nuclear Data Tables*, 92(3):375–406, 2006.

[30] Amund Tveit. A survey of agent-oriented software engineering. Proc. of the First NTNU CSGS Conference (http://www.amundt.org), May 2001.

[31] T. Waldenmaier, J. Blümer, D.M. Gonzalez, and H. Klages. Measurement of the air fluorescence yield with the airlight experiment. *Nuclear Instruments and Methods in Physics Research Section A: Accelerators, Spectrometers, Detectors and Associated Equipment*, 597(1):67–74, 2008. Proceedings of the 5th Fluorescence Workshop.

[32] T. Waldenmaier, J. Blümer, and H. Klages. Spectral resolved measurement of the nitrogen fluorescence emissions in air induced by electrons. *Astroparticle Physics*, 29(3):205–222, 2008.